Molecular genetics of the transcription factor GLIS3 identifies its dual function in beta cells and neurons

Calderari, Sophie; Ria, Massimiliano; Gérard, Christelle; Nogueira, Tatiane C.; Villate, Olatz; Collins, Stephan C.; Neil, Helen; Gervasi, Nicolas; Hue, Christophe; Suarez-zamorano, Nicolas; Prado, Cécilia; Cnop, Miriam; Bihoreau, Marie-thérèse; Kaisaki, Pamela J.; Cazier, Jean-Baptiste; Julier, Cécile; Lathrop, Mark; Werner, Michel; Eizirik, Decio L.; Gauguier, Dominique

DOI:
10.1016/j.ygeno.2017.09.001

Molecular genetics of the transcription factor GLIS3 identifies its dual function in beta cells and neurons

Sophie Calderari, Massimiliano Ria, Christelle Gérard, Tatiane C. Nogueira, Olatz Villate, Stephan C. Collins, Helen Neil, Nicolas Gervasi, Christophe Hue, Nicolas Suarez-Zamorano, Cécilia Prado, Miriam Cnop, Marie-Thérèse Bihoreau, Pamela J. Kaisaki, Jean-Baptiste Cazier, Cécile Julier, Mark Lathrop, Michel Werner, Decio L. Eizirik, Dominique Gauguier

PII: S0888-7543(17)30078-2
DOI: doi: 10.1016/j.ygeno.2017.09.001
Reference: YGENO 8918

To appear in: *Genomics*

Received date: 27 February 2017
Revised date: 8 August 2017
Accepted date: 1 September 2017

Please cite this article as: Sophie Calderari, Massimiliano Ria, Christelle Gérard, Tatiane C. Nogueira, Olatz Villate, Stephan C. Collins, Helen Neil, Nicolas Gervasi, Christophe Hue, Nicolas Suarez-Zamorano, Cécilia Prado, Miriam Cnop, Marie-Thérèse Bihoreau, Pamela J. Kaisaki, Jean-Baptiste Cazier, Cécile Julier, Mark Lathrop, Michel Werner, Decio L. Eizirik, Dominique Gauguier , Molecular genetics of the transcription factor GLIS3 identifies its dual function in beta cells and neurons, *Genomics* (2017), doi: 10.1016/j.ygeno.2017.09.001

Molecular Genetics of the Transcription Factor GLIS3 Identifies its Dual Function in Beta Cells and Neurons

Sophie Calderari[1*], Massimiliano Ria[2], Christelle Gérard[1], Tatiane C. Nogueira[3], Olatz Villate[3], Stephan C Collins[2], Helen Neil[4], Nicolas Gervasi[5], Christophe Hue[1], Nicolas Suarez-Zamorano[1], Cécilia Prado[1], Miriam Cnop[3], Marie-Thérèse Bihoreau[2], Pamela J Kaisaki[2], Jean-Baptiste Cazier[6], Cécile Julier[7], Mark Lathrop[8], Michel Werner[4$], Decio L. Eizirik[3$], Dominique Gauguier[1,2.8]

[1] Sorbonne Universities, University Pierre & Marie Curie, University Paris Descartes, Sorbonne Paris Cité, INSERM UMR_S1138, Cordeliers Research Centre, Paris, France

[2] The Wellcome Trust Centre for Human Genetics, University of Oxford, Oxford, United Kingdom

[3] ULB Center for Diabetes Research, Medical Faculty, Université Libre de Bruxelles (ULB), Brussels, Belgium

[4] FRE3377, Institut de Biologie et de Technologies de Saclay (iBiTec-S), Commissariat à l'Energie Atomique et aux Énergies Alternatives (CEA), Gif-sur-Yvette cedex, France

[5] INSERM UMR_S839, Institut du Fer à Moulin, Paris, France

[6] Centre for Computational Biology, Medical School, University of Birmingham, Birmingham, United Kingdom

[7] INSERM UMR-S 958, Faculté de Médecine Paris Diderot, University Paris 7 Denis-Diderot, Paris, Sorbonne Paris Cité, France

[8] McGill University and Genome Quebec Innovation Centre, 740 Doctor Penfield Avenue, Montreal, QC, H3A 0G1, Canada

[*] Present address: UMR BDR, INRA, ENVA, Université Paris Saclay, Jouy en Josas, France

[$] These authors contributed equally to this work.

Correspondence to Dominique Gauguier: dominique.gauguier@crc.jussieu.fr

Short title: Molecular function of GLIS3 in beta-cells and neurons

Abstract

The GLIS family zinc finger 3 isoform (GLIS3) is a risk gene for Type 1 and Type 2 diabetes, glaucoma and Alzheimer's disease endophenotype. We identified GLIS3 binding sites in insulin secreting cells (INS1) (FDR q<0.05; enrichment range 1.40-9.11 fold) sharing the motif wrGTTCCCArTAGs, which were enriched in genes involved in neuronal function and autophagy and in risk genes for metabolic and neuro-behavioural diseases. We confirmed experimentally *Glis3*-mediated regulation of the expression of genes involved in autophagy and neuron function in INS1 and neuronal PC12 cells. Naturally-occurring coding polymorphisms in *Glis3* in the Goto-Kakizaki rat model of type 2 diabetes were associated with increased insulin production *in vitro* and *in vivo*, suggestive alteration of autophagy in PC12 and INS1 and abnormal neurogenesis in hippocampus neurons. Our results support biological pleiotropy of GLIS3 in pathologies affecting β-cells and neurons and underline the existence of trans-nosology pathways in diabetes and its co-morbidities.

Keywords: Alzheimer's Disease, ChIP Sequencing, Diabetes Mellitus, Goto-Kakizaki Rat, Quantitative Trait Locus, Single Nucleotide Polymorphism

Abbreviations: AD, Alzheimer's disease; Brown Norway; ChIPseq, genome-wide chromatin immunoprecipitation sequencing; DAVID, Database for Annotation, Visualisation and Integrated Discovery; G3BS, Glis3-binding sites; GK, Goto-Kakizaki; GLIS3, GLIS family zinc finger 3 isoform; GO, Gene Ontology; GWAS, Genome-wide association studies; IPA, Ingenuity Pathway Analysis; T2D, type 2 diabetes;

1. INTRODUCTION

Genome-wide association studies (GWAS) for common inherited human diseases have shed light on novel candidate genes [1], which often lack functional characterisation to understand their role in disease pathogenesis. Growing evidence from GWAS data supports the involvement of common risk loci in diseases characterized by distinct pathophysiological features, suggesting that genes at these loci contribute to shared disease etiology through mechanisms of cross-phenotype association and pleiotropy [2, 3]. This phenomenon is illustrated with common risk loci in autoimmune and immune-mediated inflammatory diseases [4, 5], and recently extended to genetic variants shared in cancer and blood triglycerides and low-density lipoprotein cholesterol [6].

The GLIS family zinc finger 3 isoform (GLIS3) is among the most replicated GWAS signals for diabetes mellitus and related metabolic traits. It is one of the few identified GWAS risk genes for both type 1 [7-9] and type 2 [10-12] diabetes. GWAS have shown that common variants within GLIS3 itself are also associated with cerebrospinal fluid Tau [13], a biomarker in Alzheimer's disease, glaucoma [14] and serum levels of the thyroid stimulating hormone [15]. Patients with mutations in GLIS3 exhibit neonatal diabetes and congenital hypothyroidism [16, 17], but they also show a much broader spectrum of clinical manifestations, including hepatic, renal and cardiac diseases and skeletal abnormalities [16-18]. These data strongly suggest that genetic variations and mutations in GLIS3 have strong cross phenotypic effects in distinct organs.

GLIS3 is a component of Krüppel-like zinc finger transcriptional regulators that share a highly conserved five-C_2H_2-type zinc finger. It is expressed in many organs where it controls gene transcription through Glis3-binding sites (G3BS) in regulatory regions of target genes [19]. GLIS3 plays a critical role in the development and function of pancreatic β-cells, as shown for many type 2 diabetes GWAS genes [20]. Consistent with its primary etiological

role in diabetes, it regulates fasting glucose and insulin [21, 22] and glucose-stimulated insulin release [23]. *Glis3* disruption in mice causes neonatal diabetes and hypothyroidism [24-26]. *Glis3*-null pups are hyperglycemic and die prematurely. *Glis3* mutant mice exhibit small islets, with strongly decreased number of β- and δ-cells. Several studies indicate that *Glis3* indirectly regulates expression of key transcription factors (Pdx1, NeuroD1, MafA) required for the development of the endocrine pancreas and the function of mature β-cells [24, 26, 27] and is implicated in β-cell survival [28].

Despite the key role of GLIS3 in diabetes etiology and in endocrine pancreas development, molecular and cellular mechanisms mediating its function remain largely unknown. To understand diabetes-related mechanisms regulated by GLIS3 in β-cells, we carried out genome-wide chromatin immunoprecipitation sequencing (ChIPseq) of G3BS in INS1 cells, which derive from rat pancreatic β-cells, followed by molecular and physiological studies (Figure 1). Results suggest that G3BS are enriched for GWAS loci associated with metabolic diseases and neuropathologies and that GLIS3 regulates the expression of genes involved in the function of endocrine pancreas and neurons, thus suggesting cross-phenotype associations of the GLIS3 locus. Further functional studies indicate that GLIS3 exhibits dual biological roles in β-cells and neurons possibly through differential expression of autophagy genes, which provide evidence for the involvement of mechanisms of biological pleiotropy in GLIS3 function.

2. MATERIALS AND METHODS

2.1. GLIS3 chromatin immuno-precipitation and sequencing

About $1x10^7$ rat insulinoma 832/13 INS1 cells (gift from M LeGall, INSERM U872, Paris, France) were used. Proteins and DNA were cross-linked by addition of 0.4% formaldehyde (Sigma Aldrich, Saint Quentin Fallavier, France). Cells were washed with phosphate buffered saline (Sigma Aldrich, Saint Quentin Fallavier, France). Chromatin was collected by centrifugation and fragmented to generate DNA fragments of 200bp. Immunoprecipitation was performed with anti-GLIS3 antibody (Abcam, 51268, Cambridge, UK). DNA sequencing was performed on a genome analyzer GA-IIx (Illumina, Saffron Walden, UK). We obtained over 20M and about 37M reads in IP and Input, respectively. Raw sequence data have been deposited in ArrayExpress (http://www.ebi.ac.uk/arrayexpress/) under the accession number E-MTAB-5454.

Sequence alignment was performed using Bowtie. Peak calling performed with MACS2 (https://github.com/taoliu/MACS/wiki/Install-macs2) identified 299 peaks with sizes ranging from 134nt to 1656nt. Peak sequences were searched for DNA motifs using Dimont, RSAT (Peak-motifs), GimmeMotifs and completeMotifs [29]. RSAT was used on the 299 sequences restricted to the 200bp around the peak summits. Motifs were considered as significant when binomial significance $\geq$ 10. Twelve tools were considered (Mdmodule, MEME, MotifSampler, trawler, Improbizer, BioProspector, Posmo, ChIPMunk, JASPAR, AMD, HMS, GADEM). For this analysis, 90% of the full-length sequences were used to predict motifs while 10% were used to compute p-values (only motifs with a p-value < 0.001 and enrichment > 1.5 were retained). CompleteMotifs was used to combine four different tools, PATSER, MEME, Weeder and ChiPMunk. One motif with the consensus sequence wrGTTCCCArTAGs was found in the top motifs of all four tools.

2.2. Cell systems

Rat insulinoma 832/13 INS1 cells were cultured in RPMI 1640 containing 10mM HEPES, 11mM D-Glucose, 10% fetal bovine serum (FBS) (Life technologies, Saint Aubin, France), 1mM sodium pyruvate, 2mM L-glutamine, 50µM β-mercaptoethanol and maintained in 5% CO2-95% O2 at 37°C. Rat insulin-producing INS-1E cells (passages 60 to 70, gift from Dr. C. Wollheim, Geneva, Switzerland), which were derived from INS1 [30], were cultured in RPMI 1640 GlutaMAX-I (Invitrogen, Carlsbad, CA). Rat pheochromocytoma PC12 cells (Sigma Aldrich, Saint Quentin Fallavier, France) were cultured in DMEM (Life technologies, Saint Aubin, France) containing 10% horse serum and 5% fetal bovine serum (Life technologies, Saint Aubin, France). Differentiation of PC12 cells was performed in a medium containing DMEM, 1% horse serum and NGF (100ng/ml).

2.3. Animals

Colonies of Goto-Kakizaki (GK/Ox) and Brown Norway (BN) rats were bred locally. The congenic strain BN.GK-*Glis3-Ric1* (referred as BN.GK-1k throughout the text) was derived using a genetic marker assisted breeding strategy ("speed congenics") and maintained as previously described [31]. This congenic was designed to contain GK alleles at the *Glis3* locus onto the genetic background of the BN strain. Rats were allowed free access to tap water and standard laboratory chow pellets (R04-40, Safe, Augy, France) and were maintained on a 12-h light-dark cycle. All experiments were carried out with six month old male congenic and control rats. All animal procedures were performed under a UK Home Office licence approved by the ethical review panel of the University of Oxford and authorised by the Charles Darwin Ethics Committee in Animal Experiment, Paris, France.

2.4. Glucose-induced insulin secretion in vivo

Insulin secretion tests were performed by intravenous injection of glucose (0.8g /kg body wt) in rats fasted for 4 hours in the morning (post absorptive state) using the protocol applied to

the phenotypic screening of the GKxBN F2 hybrids [32]. Plasma immunoreactive insulin was assayed using an ELISA kit (Mercodia, Uppsala, Sweden).

2.5. Static incubation of pancreatic islets

BN.GK-1k congenic and BN rats were killed by cervical dislocation. Collagenase (Sigma Aldrich, Saint Quentin Fallavier, France) was rapidly injected into the ligated pancreatic duct and pancreas was excised for pancreas digestion. Islets were isolated using a stereomicroscope. Insulin secretion was measured in static incubation following overnight culture in RPMI1640 containing 5mM glucose. Groups of 10 size-matched islets were pre-incubated prior to treatment with 1, 12 and 20mM glucose. Islets were then incubated for 1 hr at 37°C and the supernatant removed for analysis. Insulin was assayed using an ELISA kit (Mercodia, Uppsala, Sweden).

2.6. Glucose-induced insulin secretion in vitro in INS1 cells

Rat insulinoma 832/13 INS1 cells were maintained in a glucose-free culture medium prior to incubation in a solution containing 2.8mM or 16.7mM of glucose. Immunoreactive insulin was determined by ELISA (Mercodia, Uppsala, Sweden) on supernatants and protein content was measured on cells.

2.7. Immunohistochemistry

Pancreata from 4-weeks old Wistar rats were fixed in 4% paraformaldehyde and embedded in paraffin. Paraffin sections (7µm) were prepared. Adjacent sections were incubated with primary antibodies: guinea-pig anti-porcine insulin (1:1000, ICN pharmaceutical, Orsay, France), rabbit antirecombinant glucagon (1:1000, Vector, Peterborough, UK) or custom made anti-rat GLIS3 (1:1000, Eurogentec, Angers, France).

2.8. Primary cultures

Hippocampi were dissected from embryonic day 18 or 19 Sprague Dawley rats. Tissue was trypsinized and neurons were plated at a density of 2.3×10^4 cells/cm^2. After attachment for

2–3 h, cells were incubated in Neurobasal medium supplemented with B27 (1×), L-glutamine (2 mM), and antibiotics (Invitrogen, Paisley, UK).

2.9. siRNA-mediated GLIS3 knock down in vitro and plasmid transfection assays

Cultured INS-1E cells were transfected with control or GLIS3 siRNA and collected for Western blot analyses for microtubule-associated protein 1 light chain 3 (LC3) -I and LC3-II protein expression. Cells were exposed or not to carbamazepine (30µM) for 24 hours and apoptosis was determined with nuclear dyes.

Glis3 cDNA from pancreatic islets were amplified from BN and GK animals and cloned into pcDNA3 (Invitrogen, Paisley, UK). INS1-cells were transfected by adding 50µl of OPTI-MEM (Life technologies, Saint Aubin, France) containing plasmid (2µg) and Lipofectamine (2µl). NGF-PC12-cells were transfected by adding 50µl of OPTI-MEM containing plasmid (1µg) and lipofectamine (1µl). Primary culture hippocampal neurons were transfected in Neurobasal medium without supplements using lipofectamine LTX with Plus Reagent (Invitrogen, Paisley, UK) and plasmid (1µg).

2.10. Imaging of cultured hippocampal neurons

Experiments were carried out with cultured hippocampal neurons 72-96 h after transfection. Imaging was obtained on a Leica SP5 confocal microscope with a 40X water objective. The number of dendrite branches crossing concentric circles around the soma was automatically counted using Fiji Sholl analysis plugin. Spine density was determined manually using single cell labelling on 3 medial branches by neuron.

2.11. Protein analyses

Total protein extracts were transferred to nitrocellulose membranes and incubated with rabbit anti-GLIS3 (1:500, Eurogentec, Angers, France), mouse anti-actin (1:5,000, #3280, Abcam, Cambridge, UK), rabbit anti-LC3 (1:500, #4108; Cell signalling, St Quentin, France), α-tubulin (1:5,000; Cell signalling, St Quentin, France). The secondary antibodies used were

horseradish peroxidase-conjugated anti-mouse antibody (1:5,000, Sigma Aldrich, Saint Quentin Fallavier, France) and anti-rabbit (1:2,000, Sigma Aldrich, Saint Quentin Fallavier, France). For autophagy analysis, total protein extracts were transferred to polyvinylidene fluoride membranes and incubated with rabbit anti-LC3 and mouse anti-actin (1:400; Abcam, Cambridge, UK). The secondary antibodies used were horseradish peroxidase-conjugated rabbit anti-goat (1:50,000; Pierce, Cramlington, UK), goat anti-rabbit antibody (1:2,000; DAKO, Ely, UK) and goat anti-mouse (1:2,000; Pierce, Cramlington, UK).

2.12. Glis3 sequencing and SNP validation

Glis3 polymorphisms were validated by sequencing genomic DNA from BN and GK strains. PolyPhen-2 v2.2.2r398 (http://genetics.bwh.harvard.edu/pph2) [33] was used to predict the potentially damaging consequences of the polymorphisms found in *Glis3*.

2.13. Real time quantitative PCR

Total RNA was prepared with RNeasy kit (Qiagen, Crawley, UK). Real-time quantitative PCR (q-PCR) was performed on a Rotor Gene 6000 (Corbett Research, Milton, UK) and the results were normalized to the house keeping gene. cDNA was amplified by real-time q-PCR with Quantitect SYBR Green PCR mastermix (Qiagen, Crawley, UK). Four to six biological replicates were analysed and each sample was analysed in triplicate. Oligonucleotides designed for PCR are given in Table S1.

2.14. Statistical analyses

Statistical analyses were performed using SPSS software version 17.0.3 (SPSS UK, Chertsey, UK). Differences in continuous variables between groups were compared using Student's *t*-tests or analysis of variance (ANOVA) with the LSD or Tamhane’s T2 test depending on whether Levene's test was insignificant or significant [$p(L) < 0.05$], respectively.

2.15. Comparative genome analysis of G3BS and relationships to GWAS

Analysis of synteny conservation between rat and human genomes was carried out for genes associated with 163 of the 169 G3BS clusters defined in Table S2. Comparative analysis of genes directly associated with GLIS3 binding sites in the rat and human genomes was used as initial anchor synteny points in the two species, which were further ascertained using the genomic position of flanking genes. We considered human orthologs flanking G3BS, and immediately adjacent genes when mapped within 100Kb of G3BS (Table S3), to search for statistically significant genetic association with diseases and disease intermediate phenotypes in the GWAS archive (www.ebi.ac.uk/gwas). All GWAS loci that we searched in this catalogue were statistically significant, ie. supported by a p-value $<1.0 \times 10^{-5}$ in the overall (initial GWAS and replication) population (www.ebi.ac.uk/gwas/docs/methods). Details of categorisation of intermediate phenotypes relevant to common diseases are given in Table S4.

2.16. Pathway analysis of genes associated with GLIS3 binding sites.

The list of genes associated with GLIS3 binding sites were submitted to Ingenuity Pathway Analysis (IPA, http://www.ingenuity.com) for pathway enrichment analysis and to the Database for Annotation, Visualisation and Integrated Discovery (DAVID, https://david.ncifcrf.gov) for gene functional annotation using Gene Ontology (GO) terms. IPA and DAVID top ranked pathways and functional group of genes to be studied were selected based on the rank, the score and the p-value. Since this is an exploratory approach, and the main pathways identified were independently validated experimentally, the p-values displayed were not corrected for multiple testing.

3. RESULTS

3.1. GLIS3-mediated transcriptional landscape in β-cells

To understand diabetes-related mechanisms regulated by GLIS3 in β-cells, we carried out genome-wide chromatin immunoprecipitation sequencing (ChIPseq) of GLIS3 binding sites (G3BS) in cultured insulin secreting INS1 cells. Read-enriched regions from the ChIP-Seq identified 299 putative G3BS ($q<0.05$; enrichment range 1.40-9.11 fold), which we grouped in 169 clusters (Table S2) evenly distributed across the genome (Figure S1). Over 65% of G3BS (195/299) and 70% of G3BS clusters (118/169) which could be mapped to the rat genome assembly were localised within 50kb of a protein coding sequence (Figure 2A). As expected, we showed that several genes close to G3BS are involved in β-cell development (*Pdx1*) and function (*Insr*, *Kcnj6*, *Slc2a2*) (Table S2). Quantitative PCR for a selection of 14 genes chosen for their tight linkage to putative G3BS validated significant chromatin enrichment for 10 loci tested (Figure S2).

Genomic sequences from the ChIP-Seq were searched for common DNA sequence motifs that could represent consensus binding sites for GLIS3. One motif with the consensus sequence, wrGTTCCCArTAGs was found in the top motifs of all four tools used (PATSER, MEME, Weeder, ChiPMunk). We confirmed the enrichment of previously proposed GLIS3 binding motifs G(T/C)CCCC(T/A)GCTGTGA(A/G) and (G/C)TGGGGGGGT(A/C) using Find Individual Motif Occurences (FIMO) and MEME [34, 35] (Table S5). Sixty-eight occurrences of the former where found in 54 peak sequences (p-value < 0.0001) and eighteen occurrences of the latter where found in 14 peak sequences (p-value < 0.0001) (Table S5). In addition, based on our sequencing data, the motif wrGTTCCCArTAGs also emerged from all software used as a new consensus DNA sequence for G3BS (Figure 2B).

3.2. Biological pathway analysis suggests dual pathophysiological role of GLIS3 in β-cells and neurons

We initially used function and pathway annotations available for genes containing or immediately adjacent to G3BS to predict functional aspects of GLIS3 biology. Results from Ingenuity Pathway Analysis (IPA) revealed its anticipated predominant role in metabolic function and diseases, even though the effects were not significant when corrected for multiple testing. A total of 60 genes associated with G3BS contributed to enrichment of functions involved in endocrine system development and function and in metabolic and endocrine system diseases (Table 1A). Interestingly, IPA also identified enrichment of functions directly relevant to other disease areas, including neurobiology through nervous system development and function (Table 1A). Results from DAVID pathway enrichment analysis (http://david.abcc.ncifcrf.gov) confirmed this finding with the identification of genes close to G3BS that contributed to statistically suggestive enrichment of the pathways synapse (*Phactr1*, *Lzts1*, *Grik1*, *Grik3*, *Erc2*, *Insr*, *Nsf*, *Itpr1*) (p=0.015), ion transport (*Trpc4*, *Kcnj6*, *Grik1*, *Slc22a12*, *Grik3*, *Kctd3*, *Abcc2*, *Muc5ac*, *Nsf*, *Kcnip4*, *Itpr1*) (p=0.008), cell projection part (*Lzts1*, *Grik1*, *Slc22a12*, *Grik3*, *Slc2a2*, *Nsf*, *Gnat3*) (p=0.008) and synaptic transmission (*Hrh1*, *Grik1*, *Grik3*, *Erc2*, *Nsf*) (p=0.049) (Table 1B). G-profiler also identified genes associated with G3BS contributing to the suggestive enrichment of the pathway neuron part (GO:0097458) (*Kcnn4*, *Nsf*, *Baiap2*, *Grik1*, *Kcnj6*, *Fam5c*, *Erc2*, *Lzts1*, *Polr2m*, *Disc1*, *Anks1a*, *Plcb4*, *Lamp5*, *Src*, *Ghrh*, *Rheb*, *Gnat3*, *Itpr1*, *Grik3*, *Ephb1*) (p=0.01). This unexpected finding obtained with insulin secreting cells INS1 is supported by co-expression of GLIS3 in brain, specifically in the hippocampus in the mouse (Figure 2C; Figure S3), and in pancreatic β-cells in the rat (Figure 2D). α-cells expressing glucagon were predominantly peripheral to the islets and evidence of co-straining for GLIS3 and insulin indicate that GLIS3 is expressed specifically in β-cells. These observations suggest that GLIS3 may also have a role in neuronal function and in diseases of the nervous system. Analysis of GLIS3

expression in the developing mouse brain supports its presence throughout hippocampal development (Figure S4).

To assess dual etiological roles of GLIS3 in metabolic and neurological diseases, we searched genes localised close to G3BS in the NHGRI-EBI catalog of published GWAS (www.ebi.ac.uk/gwas) for evidence of association with disease status and disease intermediate phenotypes. Following analysis of synteny conservation of G3BS clusters defined in Table S3 in the human genome, we identified 375 cases of genetic associations between genes at 127 G3BS and various phenotypes and disease traits (Table 2, Table S3). Interestingly, even though genetic associations to cancer phenotypes in the GWAS archive are more frequent than those to any other disease category, we found a statistically significant ($p<2.2 \times 10^{-16}$) enrichment of G3BS linked to genes associated with phenotypes relevant to cardio-metabolic diseases (n=89 for 27,982 associations; OR=6.8) and neuro-behavioural pathologies (n=72 for 15,326 associations; OR=10.1) when compared to cancer (n=23 for 49,324 associations). In a large number of cases (27), there was consistent association between genes at G3BS and both cardio-metabolic and neuropathological phenotypes. This finding was particularly significant for prime candidates for diabetes (*Pdx1*) or schizophrenia and Alzheimer's disease (*Disc1*) and replicated signals for different traits (eg. *Macrod2*, *Grik1*) (Table 2).

3.3. GLIS3 regulates gene transcription in β-cells and neurons

To provide experimental evidence for GLIS3-mediated transcriptional regulation of genes associated with G3BS and to test the hypothesis that G3BS signals originally detected in insulin secreting cells also function in neurons, GLIS3 overexpression experiments were performed with INS1 cells and with PC12 cells, which derive from a pheochromocytoma of the rat adrenal medulla and can differentiate into neurons upon NGF stimulation. We selected candidate genes for quantitative RT-PCR analysis on the basis of two criteria: their

association or close physical proximity to a putative G3BS and their known functional role in these cell types. GLIS3 stimulated expression in INS1 was associated with significant overexpression of *Ap3s1*, *Stxbp4*, *Bicd1* and *Nxph2* and reduced expression of *Atg7*, *Angptl3*, *Disc1*, *Dock7*, *Slit3* and *Fbxw11* (Figure 3A). Replication of statistically significant gene transcription changes in neuronal cells PC12 stimulated by GLIS3 was limited to downregulated expression of *Disc1* (Figure 3B). *Dock7* was also downregulated by GLIS3 in both INS1 and PC12, but the differences were not significant in PC12 cells. On the other hand, GLIS3 stimulation was associated with significantly enhanced transcription of *Atg4a* (Figure 3B), which was not evidenced in INS1 (Figure 3A). These results indicate that GLIS3 regulates gene transcription in both β-cells and neurons. Even though different collections of genes may be controlled by GLIS3 in the two cell types, our data suggest convergence to autophagy mechanisms through different genes in β-cells (*Atg7*) and neurons (*Atg4a*).

3.4. Glis3 regulates the expression of genes involved in autophagy

Results from pathway analysis also pointed to molecular mechanisms that may explain cross phenotype association mediated by GLIS3. Using DAVID (http://david.abcc.ncifcrf.gov), we showed that *Atg4c*, *Atg7* and *Atg12*, which contain, or are immediately adjacent to, G3BS contributed to suggestive enrichment of the pathway autophagy (GO:0006914; Enrichment Score 1.46; p=0.01) (Table 1), a fundamental mechanism that degrades cytoplasm constituents. The pathway regulation of autophagy in KEGG (rno04140) was also the top ranking pathway enriched when analyses were carried out with DAVID (p=0.018) and G-profiler (p=0.05). GLIS3-mediated regulation of autophagy in both β-cells and neurons was supported by cell-specific GLIS3-reactive transcription of *Atg7* and *Atg4a* in INS1 and PC12 (Figure 3A,B).

To establish the regulatory role of GLIS3 in autophagy, we initially quantified autophagic markers LC3-I and LC3-II in INS1 and PC12 overexpressing *Glis3* (Figure 3C,D).

Stimulated expression of *Glis3* was associated with significantly increased LC3-II abundance and in LC3-II/LC-I ratio in INS1 cells (Figure 3C), suggesting enhanced autophagy. We subsequently repeated the experiment in INS-1E cells treated with siRNA designed to downregulate *Glis3* expression. Transfection of INS-1E cells by siRNA targeting *Glis3* resulted in a 50% reduction in Glis3 mRNA level (Figure 3E). SiRNA-mediated GLIS3 knock-down was associated with a significant decrease in abundance of LC3-I and LC3-II (Figure 3E). In contrast, stimulated expression of *Glis3* in PC12 cells was associated with significant reduction of both abundance of LC3-I and LC3-II and conversion of LC3-I to LC3-II (Figure 3D). To examine whether stimulating autophagic flux would protect beta-cells, we used the autophagy-enhancing drug carbamazepine [36], which may promote increased clearance of autophagosomes [37]. Carbamazepine had no effects on apoptosis in INS-1E cells treated with control siRNA, but was associated with significant protection of INS-1E cells from apoptosis secondary to *Glis3* knock down. These results indicate that defective autophagy indeed contributes to cell death observed in the context of *Glis3* inhibition (Figure 3F).

3.5. Naturally-occurring polymorphisms in Glis3 affect gene expression and autophagy regulation in β-cells and neurons

Using our published genome sequence data in the Goto-Kakizaki (GK) rat model of type 2 diabetes [38], we identified two non-synonymous naturally-occurring polymorphisms (R356C and S851P) in the *Glis3* sequence (Figure S5a). Variants R356C and S851P were respectively predicted as probably and possibly damaging by the PolyPhen-2 program (http://genetics.bwh.harvard.edu/pph2/) (Figure S5b,c). The variant R356C is located in exon 13 in a region controlling GLIS3 stability through its interaction with Cullin 3 [39]. We initially tested the molecular consequences of the non synonymous variants in INS1 and PC12 neuronal cells transfected by the GK or the reference (Brown Norway, BN) allele of

Glis3. Transcription patterns of *Fbxw11*, *Disc1*, *Dock7*, *Atg7* and *Nxph2* were similar in INS1 cells transfected with GK and control alleles of *Glis3*, whereas the GK allele of *Glis3* induced marked downregulation of the expression of *Atg4a, Baiap2, Otop2 and Phactr1* ($p<0.05$), a gene associated with coronary artery disease (Figure 4A). GLIS3-mediated expression regulation of *Disc1* and *Znrf2* in PC12 cells was not affected by the GK *Glis3* variants. In contrast, transfection of GK *Glis3* in PC12 cells induced strong transcription changes of *Atg7*, *Bicd1*, *Lamp5*, *Nxph2* and *Baiap2*, a gene encoding a brain-specific protein involved in insulin signalling [40] and neurodegenerative disease [41]. In addition, GLIS3-reactive expression of *Atg4a* was abolished in these cells (Figure 4B).

We then investigated the potential impact of *Glis3* naturally occurring variants in autophagy. Stimulatory effect of GLIS3 on LC3-II abundance and in LC3-II/LC-I ratio in INS1 cells remained significant when cells were transfected by GK allele of *Glis3* (Figure 4C) as previously observed with BN *Glis3* alleles (Figure 3C). In contrast, transfection of the GK allele of *Glis3* in PC12 cells induced a sharp increase in the expression of LC3-I and LC3-II (Figure 4D), which contrasts with the inhibitory effect of the wild type allele of *Glis3* on these markers in these cells (Figure 3D).

We further complemented functional aspects of GLIS3 established in cell lines with ex vivo data derived from primary cultures of hippocampus neurons and pancreatic islets and in vivo experiments in congenic rats.

3.6. Effects of naturally-occurring polymorphisms in Glis3 on insulin secretion and neuron architecture

To test the impact of GK DNA variants in *Glis3* and associated gene transcription changes on insulin secretion and neuronal structural features, INS1 cells and primary cultures of rat hippocampus neurons were transfected by clones expressing the reference (BN) or GK allele of *Glis3*. Transfection of the GK allele of *Glis3* led to increased basal production of insulin,

which is a classical phenotypic feature observed in the GK strain, and to blunted stimulation of insulin secretion in response to a glucose challenge *in vitro* (Figure 5A), thus confirming the functional role of these variants on insulin secretion. Reduced stimulated insulin secretion (16.7mM glucose) in INS1 cells transfected with the GK allele of *Glis3* was marginally significant ($p<0.05$) when compared to glucose-stimulated untransfected INS1. Transfection of BN Glis3 had no morphological effects in neurons (Figure 5B,C), which contrasts with the effect of Glis3 in PC12, probably due to differences in cell systems used. In contrast, stimulated expression of GK *Glis3* led to significant reduction in neuron soma size (Figure 5B,C). We carried out further quantitative analysis of neuron morphology using the Sholl method, which determines the number of dendrite intersections for gradually increasing concentric circles from the soma centre. We were able to demonstrate that the GK variants of *Glis3* are associated with significant reduction of both dendritic complexity (Figure 5D) and spine density (Figure 5E), which are key neuronal features in neurodegenerative diseases. These data support the biological role of *Glis3* in the regulation of gene expression in neurons and demonstrate the strong impact of GK naturally occurring polymorphisms on β-cell function and on neurite growth and morphology.

3.7. The GK haplotype in BN.GK-1k congenics is associated with enhanced insulin secretion in vitro and in vivo and suggestive evidence of increased autophagy in brain and in pancreas

To further validate our findings in an *in vivo* system, we analysed glucose-induced insulin secretion and autophagy in rats of the congenic strain BN.GK-1k, which contains a short genomic region of chromosome 1 (1.31Mb) of GK origin, including *Glis3* and 13 additional genes, introgressed onto the genomic background of the BN strain (Figure 6A). Rats of the congenic strain exhibited a modest but statistically significant ($p<0.01$) increase in insulin secretion in response to glucose *in vivo* (Figure 6B). Basal insulin levels *in vivo* and *in vitro*

in isolated islets were similar in BN.GK-1k and BN rats (Figure 6B,C). *In vitro* insulin secretion by islets isolated from BN rats was stimulated by 12mM and 20mM glucose. Glucose stimulated insulin secretion *in vitro* by incubated islets was higher in BN.GK-1k congenic rats than in BN controls and this effect was statistically significant ($p<0.05$) in response to 20mM glucose (Figure 6C).

We then analysed markers of autophagy in total pancreas and whole brain in BN, GK and BN.GK-1k rats. Conversion of LC3 was significantly increased in GK pancreas ($p=0.0001$) and brain ($p=0.04$) when compared to BN controls (Figure 6D,E). This effect was replicated in BN.GK-1k congenic rats, which exhibited significantly higher conversion of LC3 than BN controls in both pancreas ($p=0.023$) and brain ($p=0.019$) (Figure 6D,E). The effect of GK variants of *Glis3* on the stimulation of autophagy is conserved in the pancreas and whole brain of GK and congenic rats (Fig 6D,E), whereas discordant results are obtained in INS1 and PC12 transfected with the GK alleles of *Glis3* (fig3C,D), suggesting differential regulation at the organ level and in cultured cells.

Collectively, these data provide *in vivo* experimental validation of our *in vitro* results and suggest that *Glis3* variants may account for GK phenotypes originally mapped in GKxBN F2 cross.

4. Discussion

We have established a genome-wide inventory of DNA binding sites for the transcription factor GLIS3 in insulin secreting cells, which were often located in the close vicinity of loci associated with metabolic and neurological disorders in GWAS and genes involved in autophagy and neuron function. We confirmed experimentally the role of GLIS3 on gene transcription in β-cells and neurons. Naturally-occurring non synonymous variants in *Glis3* in the GK model of type 2 diabetes (T2D) were associated with enhanced insulin secretion *in vivo* and *in vitro*, deteriorated morphology of hippocampus neurons, differential expression of key autophagy genes in insulin secreting cells and in neurons and up-regulated autophagy marker in brain and pancreas.

Genome-wide occupancy data of GLIS3 in INS1 cells allowed prediction of a comprehensive collection of target genes of this transcription factor, which complements information from gene expression studies in experimental systems. Our data confirm the documented regulation of SLC2A2 [28, 42], which occurs through its direct interaction with DNA elements at this locus. The existence of G3BS at the PDX1 locus is consistent with data from our group showing that GLIS3 regulates PDX1 expression [28], but contradicts other reports that failed to show an effect of GLIS3 on PDX1 expression [35, 42]. In addition, we did not find evidence of statistically significant enrichment of G3BS for genes known to be regulated by GLIS3 (insulin, neurogenin 3, cyclin D2) [26, 42, 43]. In particular, we were unable to replicate significant enrichment for G3BS sequences identified by electrophoretic mobility shift assay (EMSA) upstream genes encoding insulin [26, 35] and neurogenin 3 [43], which may be explained by differences in cellular material and in experimental procedures used in the studies. These may also explain the lack of G3BS identified in our study close to the vast majority of genes shown to be regulated by GLIS3 [26, 35, 42] and differentially expressed in

pancreas of Glis3 mutant mice [26], suggesting that a proportion of the transcriptional effects of GLIS3 may be species specific or indirect consequences of Glis3 inactivation.

Enriched DNA occupancy of GLIS3 at risk loci associated with metabolic and neurological diseases in GWAS supports frequent observations of genomic co-localization of risk genes for diseases characterised by distinct pathogeneses and target organs. This phenomenon of cross phenotype association [2] is well illustrated with T2D which shares common risk loci with autoimmune diseases [5], Crohn's diseases [3], osteoporosis [44] and Alzheimer's disease (AD) [13, 45]. Even though causal relationship between T2D and AD is debated [46], T2D is a risk factor for AD and etiological connections between these diseases are supported by epidemiological and experimental evidence of mechanistic relationships [47, 48]. Patients with T2D have an increased risk of developing depression and AD when compared to individuals without T2D [49] and T2D is associated with more severe cognitive impairment in Parkinson disease [50]. Reciprocally, 80% of AD patients have glucose intolerance or T2D [49] and patients with schizophrenia exhibit greater risk of developing diabetes [51]. The identification of GLIS3 variants associated with diabetes and with an AD endophenotype [13], evidence of mental impairment in GLIS3 mutated patients [16, 17] and unpublished transcriptome data suggesting GLIS3 overexpression in hippocampus of patients with dementia (http://tinyurl.com/j83hcby), indicate that GLIS3 is highly relevant to the concept of cross phenotype association and shared etiology of complex diseases. Remarkably, the risk SNPs in GLIS3 associated with diabetes (type 1 and type 2) and related traits are not in linkage disequilibrium and therefore are independent from the SNP associated with AD endophenotype, suggesting that distinct GLIS3-reactive mediators may regulate metabolic and neurological traits.

Pathway analysis of genes associated with G3BS suggested a potential role of *Glis3* in neuropathologies and in autophagy. Even though pathway enrichment was not significant

when corrected for multiple testing, and the significance of the effects was therefore only suggestive, these analyses provided functional information and raised hypotheses that can be tested experimentally. Transcription regulation of key genes involved in these pathways was analysed experimentally following *Glis3* transfection in insulin-secreting (INS1) and neuronal (PC12) cells. Even though patterns of gene transcription in response to GLIS3 stimulation are generally conserved in INS1 and PC12, DISC1 is the only GLIS3 target significantly differentially expressed in both systems. This suggests different chromatin conformation at the tested loci in β-cells and neurons and the involvement of different mediators in these cells, which may have specific physiological consequences.

Down-regulated expression of *Disc1* upon *Glis3* overexpression was a striking illustration of the conserved role of *Glis3* in β-cells and neurons. DISC1 regulates neuronal development and synapse formation [52, 53] and DISC1 variants have been consistently implicated in schizophrenia, bipolar disorder, major depression and autism [52]. Interestingly, *Disc1* downregulation in mice results in decreased β-cell proliferation, glucose intolerance, reduced insulin secretion and *Pdx1* expression [54]. Other genes involved in neuron function and neuropathologies (*Grik1, Grik3, Ube3a*, *Grinl1a, Sptlc1, Dyrk1a, Rimklb*) are associated with G3BS and contribute to enrichment of the neuron biological pathway. Glutamate receptors GRIK1 and GRIK3 modulate synaptic transmission and are associated with epilepsy, schizophrenia, AD and depressive disorder [55]. The E3 ubiquitin ligase UBE3A is critical for the processes of learning, memory and synaptic plasticity, and deficient expression of the maternal copy in the brain causes Angleman Syndrome, a neurodevelopmental disorder combining intellectual disability and seizures [56]. GRINL1A, SPTLC1 and DYRK1A are differentially expressed in brain of patients with AD [57-59] and RIMKLB is involved in schizophrenia through the regulation of N-acetyl-aspartylglutamate synthesis [60].

Autophagy is a common mechanism in β-cells and neurons in diabetes and neuropathologies. Enhanced autophagy is associated with β-cell death in T2D [61] and may protect β-cells against palmitate-induced apoptosis [37]. It suppresses neurite degeneration in PC12 cells [62] and has a neuroprotective role in AD [63]. These data suggest context-dependent regulation of autophagy in β-cells and neurons and may explain the broad and contrasting effects of GLIS3 stimulation on autophagy marker LC3II/I in INS1 and PC12 in the present study, which remains to be further characterised by the analysis of autophagy flux. The most significant autophagy gene which is differentially regulated in GLIS3 transfection experiments is ATG7, an essential component in autophagosome formation. Investigations in organ-specific *Atg7* knock-out mice demonstrated its causative role in glucose intolerance, impaired islet structure and neurodegenerative symptoms [64]. The *Pdx1* deficient mouse model of reduced insulin secretion and β-cell mass also exhibits increased autophagy [65]. The function we propose for GLIS3 in the control of autophagy underlines the complex interplay between cellular mechanisms of recycling or elimination of proteins and cytoplasmic organelles [66] in diabetes and neurodegenerative diseases, including retromer, a cellular mechanism of protein recycling from vacuolar endosomes [67] involving risk genes (SORCS1, VPS10) for T2D and AD [68, 69], and apoptosis which is stimulated by *Glis3* knock-down in INS1 and primary β-cells [28].

Analysis of the functional consequences of amino-acid changes in GLIS3 caused by GK naturally occurring genetic polymorphisms provided evidence of consistent increased autophagy markers LC3II/I in both rat brain and pancreas. Contrasting effects of GLIS3 on LC3 levels in INS1 and PC12 coincide with differential transcriptional response of *Atg7* and *Atg4a* to stimulation by the BN or GK alleles of *Glis3* in these cells, which suggests the involvement of different molecular mediators in GLIS3 function in these cells. Genetic polymorphisms in *Glis3* have also been reported in the NOD mouse model of T1D to

contribute to β-cell mass reduction and increased β-cell apoptosis in this strain [70]. In the GK rat, the variants R356C and S851P in GLIS3 may account for the quantitative trait locus for enhanced insulin secretion which we identified in a GKxBN F2 cross to a region of chromosome 1 encompassing *Glis3* [32], validated in the congenics BN.GK-*Nidd/gk1* [31], and fine mapped both in an intercross from BN.GK-Nidd/gk1 rats [71] and in the congenic strain BN.GK-1k in the present study. Their possible roles on increased autophagy in pancreas and brain remain to be replicated in β-cells and in hippocampus in BN.GK-1k and in substrains narrowing the congenic interval to *Glis3*. These variants may also account for brain anomalies suggesting neurodegeneration in the GK rat, including neuronal loss in the cerebral cortex [72] and decreased dendritic spine density in the hippocampus [73].

Increased autophagy and co-occurring enhanced insulin secretion mediated by GK GLIS3 variants may represent a mechanism observed in starved INS1 cells [74] that compensates for dramatic β-cell mass reduction in GK rats. We cannot rule out a contribution of other variants in the 1.31Mb GK segment in BN.GK-1k to the regulation of insulin secretion and autophagy. Results from our genome sequencing of the GK/ox colony [38] identified over 3,400 DNA polymorphisms in the GK genomic interval of the congenic strain BN.GK-1k (Table S6), including four non synonymous variants in AK3 (L123Q), RCL1 (S400I), JAK2 (T469R) and RLN1 (S126G), which might impact phenotypic features of BN.GK-1k rats. Collectively, results from both cell transfection with GK *Glis3* and phenotype analyses in BN.GK-1k support cross-phenotype associations of GLIS3 in GWAS for metabolic diseases and neuropathologies.

5. Conclusions

Our results provide experimental evidence for a pleiotropic role of GLIS3 in diabetes and neuropathologies and its function in β-cells and neurons. These findings require validation through replication of the ChIPseq experiment with other GLIS3 antibodies and other β-cell

models, and further functional characterisation of GLIS3, including deeper analyses of autophagy mechanisms by measuring autophagy flux. Our data suggest that GLIS3 may be a central regulatory hub for trans-nosology drug development, which may have important implications in the treatment of diabetes and its comorbidities.

ACKNOWLEDGMENTS

DG acknowledges support from a Wellcome Trust senior fellowship in basic biomedical science (057733), the European Fundation for the Study of Diabetes (EFSD), the Fondation pour le Recherche Médicale (FRM) and the Agence Nationale pour la Recherche (ANR-08-GENOPAT-030). MR was supported by a Marie Curie fellowship (PIEF-GA-2008-221255) of the European Commission. This work was supported by grants from the European Community Seventh Framework Programme (FP7/2007-2013) under grant agreements N° HEALTH-F4-2010-241504 (EURATRANS) to DG and N° HEALTH-F2-2011-277713 (BetaBat) to DLE and MC. DLE acknowledges support from the Fonds National de la Recherche Scientifique (FNRS, Belgium), Actions de Recherche Concertée de la Communauté Française (ARC, Belgium). The funding bodies had no role in the design, analysis or interpretation of this study.

REFERENCES

[1] T.A. Manolio, Genomewide association studies and assessment of the risk of disease, N Engl J Med, 363 (2010) 166-176.
[2] N. Solovieff, C. Cotsapas, P.H. Lee, S.M. Purcell, J.W. Smoller, Pleiotropy in complex traits: challenges and strategies, Nat Rev Genet, 14 (2013) 483-495.
[3] S. Sivakumaran, F. Agakov, E. Theodoratou, J.G. Prendergast, L. Zgaga, T. Manolio, I. Rudan, P. McKeigue, J.F. Wilson, H. Campbell, Abundant pleiotropy in human complex diseases and traits, Am J Hum Genet, 89 (2011) 607-618.
[4] C. Cotsapas, B.F. Voight, E. Rossin, K. Lage, B.M. Neale, C. Wallace, G.R. Abecasis, J.C. Barrett, T. Behrens, J. Cho, P.L. De Jager, J.T. Elder, R.R. Graham, P. Gregersen, L. Klareskog, K.A. Siminovitch, D.A. van Heel, C. Wijmenga, J. Worthington, J.A. Todd, D.A. Hafler, S.S. Rich, M.J. Daly, F.N.o. Consortia, Pervasive sharing of genetic effects in autoimmune disease, PLoS Genet, 7 (2011) e1002254.
[5] M.D. Fortune, H. Guo, O. Burren, E. Schofield, N.M. Walker, M. Ban, S.J. Sawcer, J. Bowes, J. Worthington, A. Barton, S. Eyre, J.A. Todd, C. Wallace, Statistical colocalization of genetic risk variants for related autoimmune diseases in the context of common controls, Nat Genet, 47 (2015) 839-846.
[6] O.A. Andreassen, V. Zuber, W.K. Thompson, A.J. Schork, F. Bettella, S. Djurovic, R.S. Desikan, I.G. Mills, A.M. Dale, P. Consortium, C. GWAS, Shared common variants in prostate cancer and blood lipids, Int J Epidemiol, 43 (2014) 1205-1214.
[7] C. Winkler, J. Krumsiek, F. Buettner, C. Angermuller, E.Z. Giannopoulou, F.J. Theis, A.G. Ziegler, E. Bonifacio, Feature ranking of type 1 diabetes susceptibility genes improves prediction of type 1 diabetes, Diabetologia, 57 (2014) 2521-2529.
[8] T. Awata, H. Yamashita, S. Kurihara, T. Morita-Ohkubo, Y. Miyashita, S. Katayama, E. Kawasaki, S. Tanaka, H. Ikegami, T. Maruyama, A. Shimada, K. Takahashi, Y. Kawabata, T. Kobayashi, N. Nishida, Y. Mawatari, A low-frequency GLIS3 variant associated with resistance to Japanese type 1 diabetes, Biochemical and biophysical research communications, 437 (2013) 521-525.
[9] J.C. Barrett, D.G. Clayton, P. Concannon, B. Akolkar, J.D. Cooper, H.A. Erlich, C. Julier, G. Morahan, J. Nerup, C. Nierras, V. Plagnol, F. Pociot, H. Schuilenburg, D.J. Smyth, H. Stevens, J.A. Todd, N.M. Walker, S.S. Rich, Genome-wide association study and meta-analysis find that over 40 loci affect risk of type 1 diabetes, Nat Genet, 41 (2009) 703-707.
[10] K.W. Hong, M. Chung, S.B. Cho, Meta-analysis of genome-wide association study of homeostasis model assessment beta cell function and insulin resistance in an East Asian population and the European results, Molecular genetics and genomics : MGG, 289 (2014) 1247-1255.
[11] Y.S. Cho, C.H. Chen, C. Hu, J. Long, R.T. Ong, X. Sim, F. Takeuchi, Y. Wu, M.J. Go, T. Yamauchi, Y.C. Chang, S.H. Kwak, R.C. Ma, K. Yamamoto, L.S. Adair, T. Aung, Q. Cai, L.C. Chang, Y.T. Chen, Y. Gao, F.B. Hu, H.L. Kim, S. Kim, Y.J. Kim, J.J. Lee, N.R. Lee, Y. Li, J.J. Liu, W. Lu, J. Nakamura, E. Nakashima, D.P. Ng, W.T. Tay, F.J. Tsai, T.Y. Wong, M. Yokota, W. Zheng, R. Zhang, C. Wang, W.Y. So, K. Ohnaka, H. Ikegami, K. Hara, Y.M. Cho, N.H. Cho, T.J. Chang, Y. Bao, A.K. Hedman, A.P. Morris, M.I. McCarthy, R. Takayanagi, K.S. Park, W. Jia, L.M. Chuang, J.C. Chan, S. Maeda, T. Kadowaki, J.Y. Lee, J.Y. Wu, Y.Y. Teo, E.S. Tai, X.O. Shu, K.L. Mohlke, N. Kato, B.G. Han, M. Seielstad, Meta-analysis of genome-wide association studies identifies eight new loci for type 2 diabetes in east Asians, Nat Genet, 44 (2012) 67-72.
[12] J. Dupuis, C. Langenberg, I. Prokopenko, R. Saxena, N. Soranzo, A.U. Jackson, E. Wheeler, N.L. Glazer, N. Bouatia-Naji, A.L. Gloyn, C.M. Lindgren, R. Mägi, A.P. Morris, J. Randall, T. Johnson, P. Elliott, D. Rybin, G. Thorleifsson, V. Steinthorsdottir, P. Henneman, H. Grallert, A. Dehghan, J.J. Hottenga, C.S. Franklin, P. Navarro, K. Song, A. Goel, J.R. Perry, J.M. Egan, T. Lajunen, N. Grarup, T. Sparsø, A. Doney, B.F. Voight, H.M. Stringham, M. Li, S. Kanoni, P. Shrader, C. Cavalcanti-Proença, M. Kumari, L. Qi, N.J. Timpson, C. Gieger, C. Zabena, G. Rocheleau, E. Ingelsson, P. An, J. O'Connell, J. Luan, A. Elliott, S.A. McCarroll, F. Payne, R.M. Roccasecca, F. Pattou, P. Sethupathy, K. Ardlie, Y.

Ariyurek, B. Balkau, P. Barter, J.P. Beilby, Y. Ben-Shlomo, R. Benediktsson, A.J. Bennett, S. Bergmann, M. Bochud, E. Boerwinkle, A. Bonnefond, L.L. Bonnycastle, K. Borch-Johnsen, Y. Böttcher, E. Brunner, S.J. Bumpstead, G. Charpentier, Y.D. Chen, P. Chines, R. Clarke, L.J. Coin, M.N. Cooper, M. Cornelis, G. Crawford, L. Crisponi, I.N. Day, E.J. de Geus, J. Delplanque, C. Dina, M.R. Erdos, A.C. Fedson, A. Fischer-Rosinsky, N.G. Forouhi, C.S. Fox, R. Frants, M.G. Franzosi, P. Galan, M.O. Goodarzi, J. Graessler, C.J. Groves, S. Grundy, R. Gwilliam, U. Gyllensten, S. Hadjadj, G. Hallmans, N. Hammond, X. Han, A.L. Hartikainen, N. Hassanali, C. Hayward, S.C. Heath, S. Hercberg, C. Herder, A.A. Hicks, D.R. Hillman, A.D. Hingorani, A. Hofman, J. Hui, J. Hung, B. Isomaa, P.R. Johnson, T. Jørgensen, A. Jula, M. Kaakinen, J. Kaprio, Y.A. Kesaniemi, M. Kivimaki, B. Knight, S. Koskinen, P. Kovacs, K.O. Kyvik, G.M. Lathrop, D.A. Lawlor, O. Le Bacquer, C. Lecoeur, Y. Li, V. Lyssenko, R. Mahley, M. Mangino, A.K. Manning, M.T. Martínez-Larrad, J.B. McAteer, L.J. McCulloch, R. McPherson, C. Meisinger, D. Melzer, D. Meyre, B.D. Mitchell, M.A. Morken, S. Mukherjee, S. Naitza, N. Narisu, M.J. Neville, B.A. Oostra, M. Orrù, R. Pakyz, C.N. Palmer, G. Paolisso, C. Pattaro, D. Pearson, J.F. Peden, N.L. Pedersen, M. Perola, A.F. Pfeiffer, I. Pichler, O. Polasek, D. Posthuma, S.C. Potter, A. Pouta, M.A. Province, B.M. Psaty, W. Rathmann, N.W. Rayner, K. Rice, S. Ripatti, F. Rivadeneira, M. Roden, O. Rolandsson, A. Sandbaek, M. Sandhu, S. Sanna, A.A. Sayer, P. Scheet, L.J. Scott, U. Seedorf, S.J. Sharp, B. Shields, G. Sigurethsson, E.J. Sijbrands, A. Silveira, L. Simpson, A. Singleton, N.L. Smith, U. Sovio, A. Swift, H. Syddall, A.C. Syvänen, T. Tanaka, B. Thorand, J. Tichet, A. Tönjes, T. Tuomi, A.G. Uitterlinden, K.W. van Dijk, M. van Hoek, D. Varma, S. Visvikis-Siest, V. Vitart, N. Vogelzangs, G. Waeber, P.J. Wagner, A. Walley, G.B. Walters, K.L. Ward, H. Watkins, M.N. Weedon, S.H. Wild, G. Willemsen, J.C. Witteman, J.W. Yarnell, E. Zeggini, D. Zelenika, B. Zethelius, G. Zhai, J.H. Zhao, M.C. Zillikens, I.B. Borecki, R.J. Loos, P. Meneton, P.K. Magnusson, D.M. Nathan, G.H. Williams, A.T. Hattersley, K. Silander, V. Salomaa, G.D. Smith, S.R. Bornstein, P. Schwarz, J. Spranger, F. Karpe, A.R. Shuldiner, C. Cooper, G.V. Dedoussis, M. Serrano-Ríos, A.D. Morris, L. Lind, L.J. Palmer, F.B. Hu, P.W. Franks, S. Ebrahim, M. Marmot, W.H. Kao, J.S. Pankow, M.J. Sampson, J. Kuusisto, M. Laakso, T. Hansen, O. Pedersen, P.P. Pramstaller, H.E. Wichmann, T. Illig, I. Rudan, A.F. Wright, M. Stumvoll, H. Campbell, J.F. Wilson, R.N. Bergman, T.A. Buchanan, F.S. Collins, K.L. Mohlke, J. Tuomilehto, T.T. Valle, D. Altshuler, J.I. Rotter, D.S. Siscovick, B.W. Penninx, D.I. Boomsma, P. Deloukas, T.D. Spector, T.M. Frayling, L. Ferrucci, A. Kong, U. Thorsteinsdottir, K. Stefansson, C.M. van Duijn, Y.S. Aulchenko, A. Cao, A. Scuteri, D. Schlessinger, M. Uda, A. Ruokonen, M.R. Jarvelin, D.M. Waterworth, P. Vollenweider, L. Peltonen, V. Mooser, G.R. Abecasis, N.J. Wareham, R. Sladek, P. Froguel, R.M. Watanabe, J.B. Meigs, L. Groop, M. Boehnke, M.I. McCarthy, J.C. Florez, I. Barroso, D. Consortium, G. Consortium, G.B. Consortium, A.H.o.b.o.P. Consortium, M. investigators, New genetic loci implicated in fasting glucose homeostasis and their impact on type 2 diabetes risk, Nat Genet, 42 (2010) 105-116.

[13] C. Cruchaga, J.S. Kauwe, O. Harari, S.C. Jin, Y. Cai, C.M. Karch, B.A. Benitez, A.T. Jeng, T. Skorupa, D. Carrell, S. Bertelsen, M. Bailey, D. McKean, J.M. Shulman, P.L. De Jager, L. Chibnik, D.A. Bennett, S.E. Arnold, D. Harold, R. Sims, A. Gerrish, J. Williams, V.M. Van Deerlin, V.M. Lee, L.M. Shaw, J.Q. Trojanowski, J.L. Haines, R. Mayeux, M.A. Pericak-Vance, L.A. Farrer, G.D. Schellenberg, E.R. Peskind, D. Galasko, A.M. Fagan, D.M. Holtzman, J.C. Morris, A.M. Goate, GWAS of cerebrospinal fluid tau levels identifies risk variants for Alzheimer's disease, Neuron, 78 (2013) 256-268.

[14] C.C. Khor, T. Do, H. Jia, M. Nakano, R. George, K. Abu-Amero, R. Duvesh, L.J. Chen, Z. Li, M.E. Nongpiur, S.A. Perera, C. Qiao, H.T. Wong, H. Sakai, M. Barbosa de Melo, M.C. Lee, A.S. Chan, Y. Azhany, T.L. Dao, Y. Ikeda, R.A. Perez-Grossmann, T. Zarnowski, A.C. Day, J.B. Jonas, P.O. Tam, T.A. Tran, H. Ayub, F. Akhtar, S. Micheal, P.T. Chew, L.A. Aljasim, T. Dada, T.T. Luu, M.S. Awadalla, N. Kitnarong, B. Wanichwecharungruang, Y.Y. Aung, J. Mohamed-Noor, S. Vijayan, S. Sarangapani, R. Husain, A. Jap, M. Baskaran, D. Goh, D.H. Su, H. Wang, V.K. Yong, L.W. Yip, T.B. Trinh, M. Makornwattana, T.T. Nguyen, E.U. Leuenberger, K.H. Park, W.A. Wiyogo, R.S. Kumar, C. Tello, Y. Kurimoto, S.S. Thapa, K. Pathanapitoon, J.F. Salmon, Y.H. Sohn, A. Fea, M. Ozaki, J.S. Lai, V. Tantisevi, C.C. Khaing, T. Mizoguchi, S. Nakano, C.Y. Kim, G. Tang, S. Fan, R. Wu, H. Meng, T.D. Tran, M. Ueno, J.M. Martinez, N. Ramli, Y.M. Aung, R.D. Reyes, S.A. Vernon, S.K. Fang, Z. Xie, X.Y. Chen, J.N. Foo, K.S. Sim, T.T. Wong, D.T. Quek, R. Venkatesh, S. Kavitha, S.R. Krishnadas, N. Soumittra, B. Shantha, B.A.

Lim, J. Ogle, J.P. de Vasconcellos, V.P. Costa, R.Y. Abe, B.B. de Souza, C.C. Sng, M.C. Aquino, E. Kosior-Jarecka, G.B. Fong, V.C. Tamanaja, R. Fujita, Y. Jiang, N. Waseem, S. Low, H.N. Pham, S. Al-Shahwan, E.R. Craven, M.I. Khan, R. Dada, K. Mohanty, M.A. Faiq, A.W. Hewitt, K.P. Burdon, E.H. Gan, A. Prutthipongsit, T. Patthanathamrongkasem, M.A. Catacutan, I.R. Felarca, C.S. Liao, E. Rusmayani, V.W. Istiantoro, G. Consolandi, G. Pignata, C. Lavia, P. Rojanapongpun, L. Mangkornkanokpong, S. Chansangpetch, J.C. Chan, B.N. Choy, J.W. Shum, H.M. Than, K.T. Oo, A.T. Han, V.H. Yong, X.Y. Ng, S.R. Goh, Y.F. Chong, M.L. Hibberd, M. Seielstad, E. Png, S.J. Dunstan, N.V. Chau, J. Bei, Y.X. Zeng, A. Karkey, B. Basnyat, F. Pasutto, D. Paoli, P. Frezzotti, J.J. Wang, P. Mitchell, J.H. Fingert, R.R. Allingham, M.A. Hauser, S.T. Lim, S.H. Chew, R.P. Ebstein, A. Sakuntabhai, J. Ahn, G. Boland, H. Snippe, R. Stead, R. Quino, S.N. Zaw, U. Lukasik, R. Shetty, M. Zahari, H.W. Bae, N.L. Oo, T. Kubota, A. Manassakorn, W.L. Ho, L. Dallorto, Y.H. Hwang, C.A. Kiire, M. Kuroda, Z.E. Djamal, J.I. Peregrino, A. Ghosh, J.W. Jeoung, T.S. Hoan, N. Srisamran, T. Sandragasu, S.H. Set, V.H. Doan, S.S. Bhattacharya, C.L. Ho, D.T. Tan, R. Sihota, S.C. Loon, K. Mori, S. Kinoshita, A.I. Hollander, R. Qamar, Y.X. Wang, Y.Y. Teo, E.S. Tai, C. Hartleben-Matkin, D. Lozano-Giral, S.M. Saw, C.Y. Cheng, J.C. Zenteno, C.P. Pang, H.T. Bui, O. Hee, J.E. Craig, D.P. Edward, M. Yonahara, J.M. Neto, M.L. Guevara-Fujita, L. Xu, R. Ritch, A.T. Liza-Sharmini, T.Y. Wong, S. Al-Obeidan, N.H. Do, P. Sundaresan, C.C. Tham, P.J. Foster, L. Vijaya, K. Tashiro, E.N. Vithana, N. Wang, T. Aung, Genome-wide association study identifies five new susceptibility loci for primary angle closure glaucoma, Nat Genet, 48 (2016) 556-562.

[15] E. Porcu, M. Medici, G. Pistis, C.B. Volpato, S.G. Wilson, A.R. Cappola, S.D. Bos, J. Deelen, M. den Heijer, R.M. Freathy, J. Lahti, C. Liu, L.M. Lopez, I.M. Nolte, J.R. O'Connell, T. Tanaka, S. Trompet, A. Arnold, S. Bandinelli, M. Beekman, S. Böhringer, S.J. Brown, B.M. Buckley, C. Camaschella, A.J. de Craen, G. Davies, M.C. de Visser, I. Ford, T. Forsen, T.M. Frayling, L. Fugazzola, M. Gögele, A.T. Hattersley, A.R. Hermus, A. Hofman, J.J. Houwing-Duistermaat, R.A. Jensen, E. Kajantie, M. Kloppenburg, E.M. Lim, C. Masciullo, S. Mariotti, C. Minelli, B.D. Mitchell, R. Nagaraja, R.T. Netea-Maier, A. Palotie, L. Persani, M.G. Piras, B.M. Psaty, K. Räikkönen, J.B. Richards, F. Rivadeneira, C. Sala, M.M. Sabra, N. Sattar, B.M. Shields, N. Soranzo, J.M. Starr, D.J. Stott, F.C. Sweep, G. Usala, M.M. van der Klauw, D. van Heemst, A. van Mullem, S.H. Vermeulen, W.E. Visser, J.P. Walsh, R.G. Westendorp, E. Widen, G. Zhai, F. Cucca, T.J. Deary, J.G. Eriksson, L. Ferrucci, C.S. Fox, J.W. Jukema, L.A. Kiemeney, P.P. Pramstaller, D. Schlessinger, A.R. Shuldiner, E.P. Slagboom, A.G. Uitterlinden, B. Vaidya, T.J. Visser, B.H. Wolffenbuttel, I. Meulenbelt, J.I. Rotter, T.D. Spector, A.A. Hicks, D. Toniolo, S. Sanna, R.P. Peeters, S. Naitza, A meta-analysis of thyroid-related traits reveals novel loci and gender-specific differences in the regulation of thyroid function, PLoS Genet, 9 (2013) e1003266.

[16] V. Senee, C. Chelala, S. Duchatelet, D. Feng, H. Blanc, J.C. Cossec, C. Charon, M. Nicolino, P. Boileau, D.R. Cavener, P. Bougneres, D. Taha, C. Julier, Mutations in GLIS3 are responsible for a rare syndrome with neonatal diabetes mellitus and congenital hypothyroidism, Nat Genet, 38 (2006) 682-687.

[17] P. Dimitri, A.M. Habeb, F. Garbuz, A. Millward, S. Wallis, K. Moussa, T. Akcay, D. Taha, J. Hogue, A. Slavotinek, J.K. Wales, A. Shetty, D. Hawkes, A.T. Hattersley, S. Ellard, E. De Franco, Expanding the clinical spectrum associated with GLIS3 mutations, J Clin Endocrinol Metab, (2015) jc20151827.

[18] P. Dimitri, J.T. Warner, J.A. Minton, A.M. Patch, S. Ellard, A.T. Hattersley, S. Barr, D. Hawkes, J.K. Wales, J.W. Gregory, Novel GLIS3 mutations demonstrate an extended multisystem phenotype, Eur J Endocrinol, 164 (2011) 437-443.

[19] Y.S. Kim, G. Nakanishi, M. Lewandoski, A.M. Jetten, GLIS3, a novel member of the GLIS subfamily of Kruppel-like zinc finger proteins with repressor and activation functions, Nucleic Acids Res, 31 (2003) 5513-5525.

[20] J. Taneera, S. Lang, A. Sharma, J. Fadista, Y. Zhou, E. Ahlqvist, A. Jonsson, V. Lyssenko, P. Vikman, O. Hansson, H. Parikh, O. Korsgren, A. Soni, U. Krus, E. Zhang, X.J. Jing, J.L. Esguerra, C.B. Wollheim, A. Salehi, A. Rosengren, E. Renström, L. Groop, A systems genetics approach identifies genes and pathways for type 2 diabetes in human islets, Cell Metab, 16 (2012) 122-134.

[21] J. Dupuis, C. Langenberg, I. Prokopenko, R. Saxena, N. Soranzo, A.U. Jackson, E. Wheeler, N.L. Glazer, N. Bouatia-Naji, A.L. Gloyn, C.M. Lindgren, R. Magi, A.P. Morris, J. Randall, T. Johnson, P.

Elliott, D. Rybin, G. Thorleifsson, V. Steinthorsdottir, P. Henneman, H. Grallert, A. Dehghan, J.J. Hottenga, C.S. Franklin, P. Navarro, K. Song, A. Goel, J.R. Perry, J.M. Egan, T. Lajunen, N. Grarup, T. Sparso, A. Doney, B.F. Voight, H.M. Stringham, M. Li, S. Kanoni, P. Shrader, C. Cavalcanti-Proenca, M. Kumari, L. Qi, N.J. Timpson, C. Gieger, C. Zabena, G. Rocheleau, E. Ingelsson, P. An, J. O'Connell, J. Luan, A. Elliott, S.A. McCarroll, F. Payne, R.M. Roccasecca, F. Pattou, P. Sethupathy, K. Ardlie, Y. Ariyurek, B. Balkau, P. Barter, J.P. Beilby, Y. Ben-Shlomo, R. Benediktsson, A.J. Bennett, S. Bergmann, M. Bochud, E. Boerwinkle, A. Bonnefond, L.L. Bonnycastle, K. Borch-Johnsen, Y. Bottcher, E. Brunner, S.J. Bumpstead, G. Charpentier, Y.D. Chen, P. Chines, R. Clarke, L.J. Coin, M.N. Cooper, M. Cornelis, G. Crawford, L. Crisponi, I.N. Day, E.J. de Geus, J. Delplanque, C. Dina, M.R. Erdos, A.C. Fedson, A. Fischer-Rosinsky, N.G. Forouhi, C.S. Fox, R. Frants, M.G. Franzosi, P. Galan, M.O. Goodarzi, J. Graessler, C.J. Groves, S. Grundy, R. Gwilliam, U. Gyllensten, S. Hadjadj, G. Hallmans, N. Hammond, X. Han, A.L. Hartikainen, N. Hassanali, C. Hayward, S.C. Heath, S. Hercberg, C. Herder, A.A. Hicks, D.R. Hillman, A.D. Hingorani, A. Hofman, J. Hui, J. Hung, B. Isomaa, P.R. Johnson, T. Jorgensen, A. Jula, M. Kaakinen, J. Kaprio, Y.A. Kesaniemi, M. Kivimaki, B. Knight, S. Koskinen, P. Kovacs, K.O. Kyvik, G.M. Lathrop, D.A. Lawlor, O. Le Bacquer, C. Lecoeur, Y. Li, V. Lyssenko, R. Mahley, M. Mangino, A.K. Manning, M.T. Martinez-Larrad, J.B. McAteer, L.J. McCulloch, R. McPherson, C. Meisinger, D. Melzer, D. Meyre, B.D. Mitchell, M.A. Morken, S. Mukherjee, S. Naitza, N. Narisu, M.J. Neville, B.A. Oostra, M. Orru, R. Pakyz, C.N. Palmer, G. Paolisso, C. Pattaro, D. Pearson, J.F. Peden, N.L. Pedersen, M. Perola, A.F. Pfeiffer, I. Pichler, O. Polasek, D. Posthuma, S.C. Potter, A. Pouta, M.A. Province, B.M. Psaty, W. Rathmann, N.W. Rayner, K. Rice, S. Ripatti, F. Rivadeneira, M. Roden, O. Rolandsson, A. Sandbaek, M. Sandhu, S. Sanna, A.A. Sayer, P. Scheet, L.J. Scott, U. Seedorf, S.J. Sharp, B. Shields, G. Sigurethsson, E.J. Sijbrands, A. Silveira, L. Simpson, A. Singleton, N.L. Smith, U. Sovio, A. Swift, H. Syddall, A.C. Syvanen, T. Tanaka, B. Thorand, J. Tichet, A. Tonjes, T. Tuomi, A.G. Uitterlinden, K.W. van Dijk, M. van Hoek, D. Varma, S. Visvikis-Siest, V. Vitart, N. Vogelzangs, G. Waeber, P.J. Wagner, A. Walley, G.B. Walters, K.L. Ward, H. Watkins, M.N. Weedon, S.H. Wild, G. Willemsen, J.C. Witteman, J.W. Yarnell, E. Zeggini, D. Zelenika, B. Zethelius, G. Zhai, J.H. Zhao, M.C. Zillikens, I.B. Borecki, R.J. Loos, P. Meneton, P.K. Magnusson, D.M. Nathan, G.H. Williams, A.T. Hattersley, K. Silander, V. Salomaa, G.D. Smith, S.R. Bornstein, P. Schwarz, J. Spranger, F. Karpe, A.R. Shuldiner, C. Cooper, G.V. Dedoussis, M. Serrano-Rios, A.D. Morris, L. Lind, L.J. Palmer, F.B. Hu, P.W. Franks, S. Ebrahim, M. Marmot, W.H. Kao, J.S. Pankow, M.J. Sampson, J. Kuusisto, M. Laakso, T. Hansen, O. Pedersen, P.P. Pramstaller, H.E. Wichmann, T. Illig, I. Rudan, A.F. Wright, M. Stumvoll, H. Campbell, J.F. Wilson, R.N. Bergman, T.A. Buchanan, F.S. Collins, K.L. Mohlke, J. Tuomilehto, T.T. Valle, D. Altshuler, J.I. Rotter, D.S. Siscovick, B.W. Penninx, D.I. Boomsma, P. Deloukas, T.D. Spector, T.M. Frayling, L. Ferrucci, A. Kong, U. Thorsteinsdottir, K. Stefansson, C.M. van Duijn, Y.S. Aulchenko, A. Cao, A. Scuteri, D. Schlessinger, M. Uda, A. Ruokonen, M.R. Jarvelin, D.M. Waterworth, P. Vollenweider, L. Peltonen, V. Mooser, G.R. Abecasis, N.J. Wareham, R. Sladek, P. Froguel, R.M. Watanabe, J.B. Meigs, L. Groop, M. Boehnke, M.I. McCarthy, J.C. Florez, I. Barroso, New genetic loci implicated in fasting glucose homeostasis and their impact on type 2 diabetes risk, Nat Genet, 42 (2010) 105-116.

[22] A. Barker, S.J. Sharp, N.J. Timpson, N. Bouatia-Naji, N.M. Warrington, S. Kanoni, L.J. Beilin, S. Brage, P. Deloukas, D.M. Evans, A. Grontved, N. Hassanali, D.A. Lawlor, C. Lecoeur, R.J. Loos, S.J. Lye, M.I. McCarthy, T.A. Mori, N.C. Ndiaye, J.P. Newnham, I. Ntalla, C.E. Pennell, B. St Pourcain, I. Prokopenko, S.M. Ring, N. Sattar, S. Visvikis-Siest, G.V. Dedoussis, L.J. Palmer, P. Froguel, G.D. Smith, U. Ekelund, N.J. Wareham, C. Langenberg, Association of genetic Loci with glucose levels in childhood and adolescence: a meta-analysis of over 6,000 children, Diabetes, 60 (2011) 1805-1812.

[23] T.W. Boesgaard, N. Grarup, T. Jorgensen, K. Borch-Johnsen, G. Meta-Analysis of, C. Insulin-Related Trait, T. Hansen, O. Pedersen, Variants at DGKB/TMEM195, ADRA2A, GLIS3 and C2CD4B loci are associated with reduced glucose-stimulated beta cell function in middle-aged Danish people, Diabetologia, 53 (2010) 1647-1655.

[24] N. Watanabe, K. Hiramatsu, R. Miyamoto, K. Yasuda, N. Suzuki, N. Oshima, H. Kiyonari, D. Shiba, S. Nishio, T. Mochizuki, T. Yokoyama, S. Maruyama, S. Matsuo, Y. Wakamatsu, H. Hashimoto, A murine model of neonatal diabetes mellitus in Glis3-deficient mice, FEBS Lett, 583 (2009) 2108-2113.

[25] Y. Yang, B.H. Chang, V. Yechoor, W. Chen, L. Li, M.J. Tsai, L. Chan, The Kruppel-like zinc finger protein GLIS3 transactivates neurogenin 3 for proper fetal pancreatic islet differentiation in mice, Diabetologia, 54 (2011) 2595-2605.
[26] H.S. Kang, Y.S. Kim, G. ZeRuth, J.Y. Beak, K. Gerrish, G. Kilic, B. Sosa-Pineda, J. Jensen, C.E. Pierreux, F.P. Lemaigre, J. Foley, A.M. Jetten, Transcription factor Glis3, a novel critical player in the regulation of pancreatic beta-cell development and insulin gene expression, Molecular and cellular biology, 29 (2009) 6366-6379.
[27] G.T. ZeRuth, Y. Takeda, A.M. Jetten, The Krüppel-like protein Gli-similar 3 (Glis3) functions as a key regulator of insulin transcription, Mol Endocrinol, 27 (2013) 1692-1705.
[28] T.C. Nogueira, F.M. Paula, O. Villate, M.L. Colli, R.F. Moura, D.A. Cunha, L. Marselli, P. Marchetti, M. Cnop, C. Julier, D.L. Eizirik, GLIS3, a susceptibility gene for type 1 and type 2 diabetes, modulates pancreatic beta cell apoptosis via regulation of a splice variant of the BH3-only protein Bim, PLoS Genet, 9 (2013) e1003532.
[29] L. Kuttippurathu, M. Hsing, Y. Liu, B. Schmidt, D.L. Maskell, K. Lee, A. He, W.T. Pu, S.W. Kong, CompleteMOTIFs: DNA motif discovery platform for transcription factor binding experiments, Bioinformatics, 27 (2011) 715-717.
[30] A. Merglen, S. Theander, B. Rubi, G. Chaffard, C.B. Wollheim, P. Maechler, Glucose sensitivity and metabolism-secretion coupling studied during two-year continuous culture in INS-1E insulinoma cells, Endocrinology, 145 (2004) 667-678.
[31] R.H. Wallis, S.C. Collins, P.J. Kaisaki, K. Argoud, S.P. Wilder, K.J. Wallace, M. Ria, A. Ktorza, P. Rorsman, M.T. Bihoreau, D. Gauguier, Pathophysiological, genetic and gene expression features of a novel rodent model of the cardio-metabolic syndrome, PLoS One, 3 (2008) e2962.
[32] D. Gauguier, P. Froguel, V. Parent, C. Bernard, M.T. Bihoreau, B. Portha, M.R. James, L. Penicaud, M. Lathrop, A. Ktorza, Chromosomal mapping of genetic loci associated with non-insulin dependent diabetes in the GK rat, Nat Genet, 12 (1996) 38-43.
[33] I.A. Adzhubei, S. Schmidt, L. Peshkin, V.E. Ramensky, A. Gerasimova, P. Bork, A.S. Kondrashov, S.R. Sunyaev, A method and server for predicting damaging missense mutations, Nat Methods, 7 (2010) 248-249.
[34] J.Y. Beak, H.S. Kang, Y.S. Kim, A.M. Jetten, Functional analysis of the zinc finger and activation domains of Glis3 and mutant Glis3(NDH1), Nucleic Acids Res, 36 (2008) 1690-1702.
[35] Y. Yang, B.H. Chang, S.L. Samson, M.V. Li, L. Chan, The Kruppel-like zinc finger protein Glis3 directly and indirectly activates insulin gene transcription, Nucleic Acids Res, 37 (2009) 2529-2538.
[36] T. Hidvegi, M. Ewing, P. Hale, C. Dippold, C. Beckett, C. Kemp, N. Maurice, A. Mukherjee, C. Goldbach, S. Watkins, G. Michalopoulos, D.H. Perlmutter, An autophagy-enhancing drug promotes degradation of mutant alpha1-antitrypsin Z and reduces hepatic fibrosis, Science, 329 (2010) 229-232.
[37] M. Cnop, B. Abdulkarim, G. Bottu, D.A. Cunha, M. Igoillo-Esteve, M. Masini, J.V. Turatsinze, T. Griebel, O. Villate, I. Santin, M. Bugliani, L. Ladriere, L. Marselli, M.I. McCarthy, P. Marchetti, M. Sammeth, D.L. Eizirik, RNA sequencing identifies dysregulation of the human pancreatic islet transcriptome by the saturated fatty acid palmitate, Diabetes, 63 (2014) 1978-1993.
[38] S.S. Atanur, A.G. Diaz, K. Maratou, A. Sarkis, M. Rotival, L. Game, M.R. Tschannen, P.J. Kaisaki, G.W. Otto, M.C. Ma, T.M. Keane, O. Hummel, K. Saar, W. Chen, V. Guryev, K. Gopalakrishnan, M.R. Garrett, B. Joe, L. Citterio, G. Bianchi, M. McBride, A. Dominiczak, D.J. Adams, T. Serikawa, P. Flicek, E. Cuppen, N. Hubner, E. Petretto, D. Gauguier, A. Kwitek, H. Jacob, T.J. Aitman, Genome Sequencing Reveals Loci under Artificial Selection that Underlie Disease Phenotypes in the Laboratory Rat, Cell, 154 (2013) 691-703.
[39] G.T. ZeRuth, X.P. Yang, A.M. Jetten, Modulation of the transactivation function and stability of Kruppel-like zinc finger protein Gli-similar 3 (Glis3) by Suppressor of Fused, J Biol Chem, 286 (2011) 22077-22089.
[40] M.Y. Heung, B. Visegrady, K. Futterer, L.M. Machesky, Identification of the insulin-responsive tyrosine phosphorylation sites on IRSp53, Eur J Cell Biol, 87 (2008) 699-708.

[41] M.H. Kim, J. Choi, J. Yang, W. Chung, J.H. Kim, S.K. Paik, K. Kim, S. Han, H. Won, Y.S. Bae, S.H. Cho, J. Seo, Y.C. Bae, S.Y. Choi, E. Kim, Enhanced NMDA receptor-mediated synaptic transmission, enhanced long-term potentiation, and impaired learning and memory in mice lacking IRSp53, J Neurosci, 29 (2009) 1586-1595.
[42] Y. Yang, B.H. Chang, L. Chan, Sustained expression of the transcription factor GLIS3 is required for normal beta cell function in adults, EMBO Mol Med, 5 (2013) 92-104.
[43] Y.S. Kim, H.S. Kang, Y. Takeda, L. Hom, H.Y. Song, J. Jensen, A.M. Jetten, Glis3 regulates neurogenin 3 expression in pancreatic beta-cells and interacts with its activator, Hnf6, Mol Cells, 34 (2012) 193-200.
[44] L.K. Billings, Y.H. Hsu, R.J. Ackerman, J. Dupuis, B.F. Voight, L.J. Rasmussen-Torvik, S. Hercberg, M. Lathrop, D. Barnes, C. Langenberg, J. Hui, M. Fu, N. Bouatia-Naji, C. Lecoeur, P. An, P.K. Magnusson, I. Surakka, S. Ripatti, L. Christiansen, C. Dalgard, L. Folkersen, E. Grundberg, P. Eriksson, J. Kaprio, K. Ohm Kyvik, N.L. Pedersen, I.B. Borecki, M.A. Province, B. Balkau, P. Froguel, A.R. Shuldiner, L.J. Palmer, N. Wareham, P. Meneton, T. Johnson, J.S. Pankow, D. Karasik, J.B. Meigs, D.P. Kiel, J.C. Florez, Impact of common variation in bone-related genes on type 2 diabetes and related traits, Diabetes, 61 (2012) 2176-2186.
[45] J.C. Bis, C. DeCarli, A.V. Smith, F. van der Lijn, F. Crivello, M. Fornage, S. Debette, J.M. Shulman, H. Schmidt, V. Srikanth, M. Schuur, L. Yu, S.H. Choi, S. Sigurdsson, B.F. Verhaaren, A.L. DeStefano, J.C. Lambert, C.R. Jack, M. Struchalin, J. Stankovich, C.A. Ibrahim-Verbaas, D. Fleischman, A. Zijdenbos, T. den Heijer, B. Mazoyer, L.H. Coker, C. Enzinger, P. Danoy, N. Amin, K. Arfanakis, M.A. van Buchem, R.F. de Bruijn, A. Beiser, C. Dufouil, J. Huang, M. Cavalieri, R. Thomson, W.J. Niessen, L.B. Chibnik, G.K. Gislason, A. Hofman, A. Pikula, P. Amouyel, K.B. Freeman, T.G. Phan, B.A. Oostra, J.L. Stein, S.E. Medland, A.A. Vasquez, D.P. Hibar, M.J. Wright, B. Franke, N.G. Martin, P.M. Thompson, M.A. Nalls, A.G. Uitterlinden, R. Au, A. Elbaz, R.J. Beare, J.C. van Swieten, O.L. Lopez, T.B. Harris, V. Chouraki, M.M. Breteler, P.L. De Jager, J.T. Becker, M.W. Vernooij, D. Knopman, F. Fazekas, P.A. Wolf, A. van der Lugt, V. Gudnason, W.T. Longstreth, M.A. Brown, D.A. Bennett, C.M. van Duijn, T.H. Mosley, R. Schmidt, C. Tzourio, L.J. Launer, M.A. Ikram, S. Seshadri, E.N.I.G.t.M.-A. Consortium, C.f.H.a.A.R.i.G.E. Consortium, Common variants at 12q14 and 12q24 are associated with hippocampal volume, Nat Genet, 44 (2012) 545-551.
[46] P. Proitsi, M.K. Lupton, L. Velayudhan, G. Hunter, S. Newhouse, K. Lin, I. Fogh, M. Tsolaki, M. Daniilidou, M. Pritchard, D. Craig, S. Todd, J.A. Johnston, B. McGuinness, I. Kloszewska, H. Soininen, P. Mecocci, B. Vellas, P.A. Passmore, R. Sims, J. Williams, C. Brayne, R. Stewart, P. Sham, S. Lovestone, J.F. Powell, A.s.D.N. Initiative, G. Consortium, Alleles that increase risk for type 2 diabetes mellitus are not associated with increased risk for Alzheimer's disease, Neurobiol Aging, 35 (2014) 2883.e2883-2883.e2810.
[47] J.A. Luchsinger, Adiposity, hyperinsulinemia, diabetes and Alzheimer's disease: an epidemiological perspective, Eur J Pharmacol, 585 (2008) 119-129.
[48] S.M. de la Monte, J.R. Wands, Alzheimer's disease is type 3 diabetes-evidence reviewed, J Diabetes Sci Technol, 2 (2008) 1101-1113.
[49] C. Toth, Diabetes and neurodegeneration in the brain, Handbook of clinical neurology, 126 (2014) 489-511.
[50] N.I. Bohnen, V. Kotagal, M.L. Muller, R.A. Koeppe, P.J. Scott, R.L. Albin, K.A. Frey, M. Petrou, Diabetes mellitus is independently associated with more severe cognitive impairment in Parkinson disease, Parkinsonism & related disorders, 20 (2014) 1394-1398.
[51] A.J. Mitchell, D. Vancampfort, K. Sweers, R. van Winkel, W. Yu, M. De Hert, Prevalence of metabolic syndrome and metabolic abnormalities in schizophrenia and related disorders--a systematic review and meta-analysis, Schizophr Bull, 39 (2013) 306-318.
[52] P.A. Thomson, E.L. Malavasi, E. Grunewald, D.C. Soares, M. Borkowska, J.K. Millar, DISC1 genetics, biology and psychiatric illness, Frontiers in biology, 8 (2013) 1-31.
[53] Z. Wen, H.N. Nguyen, Z. Guo, M.A. Lalli, X. Wang, Y. Su, N.S. Kim, K.J. Yoon, J. Shin, C. Zhang, G. Makri, D. Nauen, H. Yu, E. Guzman, C.H. Chiang, N. Yoritomo, K. Kaibuchi, J. Zou, K.M. Christian, L.

Cheng, C.A. Ross, R.L. Margolis, G. Chen, K.S. Kosik, H. Song, G.L. Ming, Synaptic dysregulation in a human iPS cell model of mental disorders, Nature, 515 (2014) 414-418.
[54] A. Jurczyk, A. Nowosielska, N. Przewozniak, K.E. Aryee, P. DiIorio, D. Blodgett, C. Yang, M. Campbell-Thompson, M. Atkinson, L. Shultz, A. Rittenhouse, D. Harlan, D. Greiner, R. Bortell, Beyond the brain: disrupted in schizophrenia 1 regulates pancreatic β-cell function via glycogen synthase kinase-3β, FASEB J, 30 (2016) 983-993.
[55] D.E. Jane, D. Lodge, G.L. Collingridge, Kainate receptors: pharmacology, function and therapeutic potential, Neuropharmacology, 56 (2009) 90-113.
[56] L.M. Bird, Angelman syndrome: review of clinical and molecular aspects, The application of clinical genetics, 7 (2014) 93-104.
[57] C.P. Jacob, E. Koutsilieri, J. Bartl, E. Neuen-Jacob, T. Arzberger, N. Zander, R. Ravid, W. Roggendorf, P. Riederer, E. Grunblatt, Alterations in expression of glutamatergic transporters and receptors in sporadic Alzheimer's disease, J Alzheimers Dis, 11 (2007) 97-116.
[58] S.E. Bergen, C.T. O'Dushlaine, S. Ripke, P.H. Lee, D.M. Ruderfer, S. Akterin, J.L. Moran, K.D. Chambert, R.E. Handsaker, L. Backlund, U. Osby, S. McCarroll, M. Landen, E.M. Scolnick, P.K. Magnusson, P. Lichtenstein, C.M. Hultman, S.M. Purcell, P. Sklar, P.F. Sullivan, Genome-wide association study in a Swedish population yields support for greater CNV and MHC involvement in schizophrenia compared with bipolar disorder, Mol Psychiatry, 17 (2012) 880-886.
[59] J. Wegiel, C.X. Gong, Y.W. Hwang, The role of DYRK1A in neurodegenerative diseases, FEBS J, 278 (2011) 236-245.
[60] F. Collard, D. Vertommen, S. Constantinescu, L. Buts, E. Van Schaftingen, Molecular identification of beta-citrylglutamate hydrolase as glutamate carboxypeptidase 3, J Biol Chem, 286 (2011) 38220-38230.
[61] M. Masini, M. Bugliani, R. Lupi, S. del Guerra, U. Boggi, F. Filipponi, L. Marselli, P. Masiello, P. Marchetti, Autophagy in human type 2 diabetes pancreatic beta cells, Diabetologia, 52 (2009) 1083-1086.
[62] Y. Yang, S. Chen, J. Zhang, C. Li, Y. Sun, L. Zhang, X. Zheng, Stimulation of autophagy prevents amyloid-β peptide-induced neuritic degeneration in PC12 cells, J Alzheimers Dis, 40 (2014) 929-939.
[63] R.A. Nixon, The role of autophagy in neurodegenerative disease, Nat Med, 19 (2013) 983-997.
[64] J. Xiong, Atg7 in development and disease: panacea or Pandora's Box?, Protein Cell, 6 (2015) 722-734.
[65] K. Fujimoto, P.T. Hanson, H. Tran, E.L. Ford, Z. Han, J.D. Johnson, R.E. Schmidt, K.G. Green, B.M. Wice, K.S. Polonsky, Autophagy regulates pancreatic beta cell death in response to Pdx1 deficiency and nutrient deprivation, J Biol Chem, 284 (2009) 27664-27673.
[66] G. Mariño, M. Niso-Santano, E.H. Baehrecke, G. Kroemer, Self-consumption: the interplay of autophagy and apoptosis, Nat Rev Mol Cell Biol, 15 (2014) 81-94.
[67] J.S. Bonifacino, J.H. Hurley, Retromer, Curr Opin Cell Biol, 20 (2008) 427-436.
[68] R.F. Lane, S.M. Raines, J.W. Steele, M.E. Ehrlich, J.A. Lah, S.A. Small, R.E. Tanzi, A.D. Attie, S. Gandy, Diabetes-associated SorCS1 regulates Alzheimer's amyloid-beta metabolism: evidence for involvement of SorL1 and the retromer complex, J Neurosci, 30 (2010) 13110-13115.
[69] R.F. Lane, P. St George-Hyslop, B.L. Hempstead, S.A. Small, S.M. Strittmatter, S. Gandy, Vps10 family proteins and the retromer complex in aging-related neurodegeneration and diabetes, J Neurosci, 32 (2012) 14080-14086.
[70] J. Dooley, L. Tian, S. Schonefeldt, V. Delghingaro-Augusto, J.E. Garcia-Perez, E. Pasciuto, D. Di Marino, E.J. Carr, N. Oskolkov, V. Lyssenko, D. Franckaert, V. Lagou, L. Overbergh, J. Vandenbussche, J. Allemeersch, G. Chabot-Roy, J.E. Dahlstrom, D.R. Laybutt, N. Petrovsky, L. Socha, K. Gevaert, A.M. Jetten, D. Lambrechts, M.A. Linterman, C.C. Goodnow, C.J. Nolan, S. Lesage, S.M. Schlenner, A. Liston, Genetic predisposition for beta cell fragility underlies type 1 and type 2 diabetes, Nat Genet, 48 (2016) 519-527.

[71] S.C. Collins, R.H. Wallis, S.P. Wilder, K.J. Wallace, K. Argoud, P.J. Kaisaki, M.T. Bihoreau, D. Gauguier, Mapping diabetes QTL in an intercross derived from a congenic strain of the Brown Norway and Goto-Kakizaki rats, Mamm Genome, 17 (2006) 538-547.
[72] S. Hussain, S. Mansouri, Å. Sjöholm, C. Patrone, V. Darsalia, Evidence for cortical neuronal loss in male type 2 diabetic Goto-Kakizaki rats, J Alzheimers Dis, 41 (2014) 551-560.
[73] Q. Xiang, J. Zhang, C.Y. Li, Y. Wang, M.J. Zeng, Z.X. Cai, R.B. Tian, W. Jia, X.H. Li, Insulin resistance-induced hyperglycemia decreased the activation of Akt/CREB in hippocampus neurons: Molecular evidence for mechanism of diabetes-induced cognitive dysfunction, Neuropeptides, 54 (2015) 9-15.
[74] A. Goginashvili, Z. Zhang, E. Erbs, C. Spiegelhalter, P. Kessler, M. Mihlan, A. Pasquier, K. Krupina, N. Schieber, L. Cinque, J. Morvan, I. Sumara, Y. Schwab, C. Settembre, R. Ricci, Insulin granules. Insulin secretory granules control autophagy in pancreatic β cells, Science, 347 (2015) 878-882.

Legends to figures

Figure 1. Outlined experimental design and methods applied to the identification of GLIS3 target genes in INS1 insulin secreting cells and the characterisation of it function.

Figure 2. Outlined output of ChIP-Seq analysis of GLIS3 binding sites (G3BS) in INS1 cells and relevance of GLIS3 and its targets to metabolic and neurobehavioural diseases. Read-enriched regions from the ChIP-Seq experiment derived with an ABCAM antibody were analysed using MACS2 (https://pypi.python.org/pypi/MACS2/) and sequences were aligned to the rat reference genome assembly (Rnor_5.0 release 74) to identify the closest gene. **a.** Profile of Glis3 marks with respect to nearby transcription start site (TSS). Input is represented by the dashed red line and the solid blue line represents the IP. **b.** Dimont, RSAT (Peak-motifs) and GimmeMotifs tools were used to search for conserved motifs in peak sequences and CompleteMotifs identified a single consensus motif sequence for G3BS. **c.** Evidence of GLIS3 expression in hippocampus assessed by in situ hybridization (source: The Allen Mouse Brain Atlas, http://mouse.brain-map.org/gene/show/86346). **d.** Localisation of GLIS3 in pancreatic islets assessed by immunocytochemistry. Serial staining (brown) of pancreas sections shows the localisation of insulin, glucagon and Glis3, using a custom made antibody (Eurogentec). Red arrow indicates an area specifically stained for glucagon and white arrows areas of staining for both GLIS3 and insulin and demonstrating co-localisation. **e.** Association of loci linked to GLIS3 binding sites with disease phenotypes in GWAS (www.ebi.ac.uk/gwas).

Figure 3. Effects of GLIS3 on the expression of genes close to G3BS and autophagy in insulin-secreting cells and neurons. Expression of genes associated with G3BS was tested by quantitative RT-PCR in INS1 (**a**) and NGF-PC12 (**b**) cells overexpressing the wild-type (Brown-Norway, BN) allele of *Glis3* (INS1-GLIS3 and PC12-GLIS3). Results are expressed

in 2-DDCT (vs GAPDH and vs controls cells transfected with empty plasmid) on 4 biological replicates. LC3-I and -II protein levels and ratio were determined in INS1 cells (**c**) and in NGF-PC12 cells (**d**) transfected with a control plasmid (INS-CTL, PC12-CTL) and with a plasmid expressing *Glis3* (INS1-GLIS3, PC12-GLIS3). SiRNA-mediated Glis3 expression knock-down in INS-1E cells and representative blots and densitometry of LC3-I and LC3-II protein expression normalized by the housekeeping protein α-tubulin in INS-1E cells transfected with control or GLIS3 siRNA (**e**). Results are means ± SEM (n = 5). Effect of carbamazepine on GLIS3 knock down-mediated apoptosis in INS1-E cells (n=7) (**f**). Results are means ± SEM. *p<0.05, **p<0.01, *** P<0.001 significantly different to controls; ### P<0.001 significantly different to siGLIS3 or $$ P<0.01 significantly different to siGLIS3 with carbamazepine.

Figure 4. Impact of *Glis3* polymorphisms on gene expression and the regulation of autophagy in insulin secreting cells and neurons. Expression of genes associated with G3BS was tested by quantitative RT-PCR in INS1 (**a**) and NGF-PC12 (**b**) cells overexpressing the wild-type (Brown-Norway, BN) allele or the GK allele of *Glis3.* Quantitative RT PCR results are expressed in 2-DDCT (vs GAPDH and vs controls cells transfected with empty plasmid) on 4 biological replicates. *p<0.05 significantly different to controls. **c.** LC3-I and -II protein levels and LC3-I to LC3-II ratio in INS1 cells transfected with a control plasmid (INS1-CTL) and with a plasmid expressing the GK allele of *Glis3* (INS1-GLIS3GK). **d.** LC3-I and -II protein levels and ratio in NGF-PC12 cells transfected with a plasmid control (PC12-CTL) and with a plasmid expressing the GK allele of *Glis3* (PC12-GLIS3GK). Data are reported as mean ± SEM based on 6 biological replicates. *p<0.05, **p<0.01 significantly different to controls.

Figure 5. Effects of naturally occurring polymorphisms of *Glis3* in the GK strain on insulin secretion in INS cells and neurite complexity in cultured hippocampus neurons.

a. Glucose stimulated insulin secretion in INS1 cells. Cells were transfected with an empty plasmid (CTL), or plasmids expressing *Glis3* alleles from either the Brown Norway control strain (GLIS3) or the diabetic GK strain (Glis3GK) (n=9 per group). Data are means ± SEM. *p<0.05, ***p<0.001 significant differences in insulin secretion between glucose concentations of 16.7mM and 2.8mM (basal). **b.** Hippocampal neurons (DIV21) were co-transfected with GFP and either control plasmids or cloned cDNAs expressing the BN or GK alleles of *Glis3*, and imaged by confocal microscopy after 5 days. **c.** Quantification of soma size. Each soma where delimited manually with ROI and the area were extracted (n=30). **d.** Sholl analysis. The number of dendrite branches crossing concentric circles around the soma was automatically counted using Fiji Sholl analysis plugin (n=30). **e.** Spine density per µm quantification. Data are means ± SEM; *p<0.05, **p<0.01 significantly different to controls.

Figure 6. *In vivo* and *in vitro* insulin secretion and autophagy in a rat congenic strain carrying GK Glis3 variants. Details of the GK genomic region (highlighted in yellow) introgressed onto a BN background in the congenic BN.GK-1k **(a)**. Glucose stimulated insulin secretion *in vivo* (**b**) and *in vitro* in isolated islets (**c**). Autophagy in total pancreas (**d**) and whole brain (**e**). Number of replicates are indicated in the bars. Data are means ± SEM; *p<0.05, **p<0.01, ***p<0.001 significantly different to BN controls.

Table 1. Biological pathway enrichment analysis of genes encompassing GLIS3 binding sites. Analyses were carried out with Ingenuity Pathway Analysis (IPA) (A) and with DAVID (B) (david.abcc.ncifcrf.gov) using Gene Ontology (GO) terms. For each pathway or function genes contributing to enrichment are given. P-values are not corrected for multiple testing. ES, Enrichment Scores.

A- Ingenuity Pathway Analysis

Top Functions (Ranking)	Score	Focus molecules
Endocrine System Development and Function, Molecular Transport, Protein Synthesis (1)	46	ABCC2, ARF1, BMP2K, DISC1, DYRK1A, EPHB1, ITPR1, KCNN4, MAN2A1, MMD, MSR1, MUC5AC, PAQR3, PDX1, PHACTR1, SLC2A2, TAF11, TRPC4, TSPAN9, VAV1, ZBTB20
Endocrine System Disorders, Metabolic Disease, Cell Morphology (2)	35	ANGPTL3, ATG7, BAIAP2, EZH2, GRIK1, GRIK3, INSR, LPHN3, LZTS1, MEOX1, NLRP12, NSF, PDX1, RP2, SLC2A2, SLIT3, STXBP4
Nervous System Development and Function, Tissue Morphology, Cancer (3)	28	ANKS1A, CGGBP1, COL14A1, ECHDC1, FAM5C, GAA, KCNG1, KCTD3, NEIL3, RIMKLB, RPS6KC1, STXBP6, ZNRF2
Endocrine System Disorders, Gastrointestinal Disease, Hereditary Disorder (4)	26	ANKRD10, ATG4C, CDO1, CGGBP1, COX15, CYB561, FAM105A, FECH, FOXP1, GALNT11, GFPT1, LRIF1, LRP5, MANBAL, SLC22A12, SPTLC1, TCOF1
Endocrine System Disorders, Metabolic Disease, Carbohydrate Metabolism (5)	24	GPR12, HSD17B6, KCNJ6, LAMP5, MAML2, PLA2G12B, PPP1R12B, SLC2A2

B- DAVID

GO id	GO Term (Cluster)	P-value	ES	Contributing genes
6914	Autophagy (1)	0.011	1.46	ATG12, ATG4C, ATG7
45202	Synapse (2)	0.016	1.43	PHACTR1, LZTS1, GRIK1, GRIK3, ERC2, INSR, NSF, ITPR1
44463	Cell projection part (3)	0.008	1.37	LZTS1, GRIK1, SLC22A12, GRIK3, SLC2A2, NSF, GNAT3
6811	Ion transport (4)	0.009	1.22	TRPC4, KCNJ6, GRIK1, SLC22A12, GRIK3, KCTD3, ABCC2, MUC5AC, NSF, KCNIP4, ITPR1
5216	Ion channel activity (4)	0.020		TRPC4, KCNJ6, GRIK1, GRIK3, KCTD3, KCNIP4, ITPR1
48878	Chemical homeostasis (4)	0.035		FECH, GRIK1, GRIK3, PDX1, ABCC2, ANGPTL3, INSR, ITPR1
5887	Integral to plasma membrane (6)	0.012	1.15	TRPC4, FLT1, GRIK1, GRIK3, KCTD3, ABCC2, INSR, EPHB1
7267	Cell-cell signaling (7)	0.017	1.06	HRH1, GRIK1, GRIK3, PDX1, ERC2, NSF, EPHB1
42995	Cell projection (7)	0.028		LZTS1, GRIK1, SLC22A12, GRIK3, BAIAP2, SLC2A2, KATNB1, RHEB, ERC2, NSF, GNAT3

7268	Synaptic transmission (7)	0.049		HRH1, GRIK1, GRIK3, ERC2, NSF
5525	GTP binding (8)	0.014	1.01	ARF2, DOCK9, RHEB, DOCK7, RAB38, INSR, GNAT3
32555	Purine ribonucleotide binding (10)	0.017	0.92	FLT1, RGD1561667, DOCK9, DOCK7, EPHB1, GNAT3, RFC3, ARF2, ASCC3, DGKG, DYRK1A, RGD1560718, BMP2K, RHEB, RAB38, ABCC2, INSR, NSF
4713	Protein tyrosine kinase activity (10)	0.040		FLT1, DYRK1A, INSR, EPHB1
6289	Nucleotide-excision repair (16)	0.039	0.78	RFC3, NEIL3, BRCA2
48878	Chemical homeostasis (19)	0.035	0.71	FECH, GRIK1, GRIK3, PDX1, ABCC2, ANGPTL3, INSR, ITPR1
31667	Response to nutrient levels (23)	0.032	0.66	ATG12, ATG7, BRCA2, PDX1, MUC5AC, INSR

Table 2. Comparative mapping analysis of GLIS3 binding sites in the human genome. Human orthologs flanking GLIS3 binding sites (G3BS) were searched in the GWAS archive (www.ebi.ac.uk/gwas) for published genetic association with diseases and phenotypes. All GWAS loci that we searched in this catalogue were statistically significant, ie. supported by a p-value $<1.0 \times 10^{-5}$ in the overall (initial GWAS and replication) population Reference to the G3BS clusters defined in Table S2 is reported in parentheses. Intermediate phenotypes were associated with relevant diseases and categorised as described in Table S4. GWAS signals for both cardio-metabolic and neurodegenerative/neurobehavioral phenotypes are underlined.

Cardio-metabolic diseases

Type 2 diabetes: SLC2A2 (28), CHL1 (52), TMEFF2 (85), PDX1/GSX1 (110), PPP2R2C (125), SPRY2 (134), UHRF1BP1 (160)

Obesity: RSPO3 (1), NLRP8 (8), c19orf18 (9), UBE3A (14), COX15 (25), TRPC4 (29), UNC5C (36), LPHN2 (37), NEGR1 (38), PAK7 (41), MACROD2 (42), CHL1 (52), ITPR1 (58), BICD1 (61), LINGO2 (62), TLR4 (63), STXBP6 (70), TRIB1 (77), FAM84B (77), MAML2 (78), EPHB1/PPP2R3A (80), TMEM100/MMD (91), TOM1L1 (92), AATK/RPTOR (98), GRIK1 (100), SETD4 (101), DGKG (105), RFC3 (107), SLC46A3 (109), DPP10 (117), PPP1R12B (118), FGFRL1 (122), KCNIP4 (128), MRPS24 (129), SPRY2 (134), NRG3 (137), DDX60L/PALLD (140), FHOD3 (148), SCGB3A2/SPINK1 (149), KCNN2 (149), RPS14 (151), CAMK2A (151), ANKS1A (160), GRIK2 (163)

Adipose tissue variables: ADCY2 (2), ARRDC4 (16), NEGR1 (38), FOXP1 (57), TRIB1 (77), FER (86), BACH1 (100)

Insulin resistance and metabolic syndrome: DYRK1A (102), INSR (108), ZNF644 (123), GAS1 (145), TOX3 (157)

Lipid metabolism: PAPD7 (2), Cd36 (50), PRMT8 (60), TRIB1 (77), RUNX1 (101), ATP6V1B2/SLC18A1 (139), LPAR2 (139), CNTNAP4 (158)

Cardiovascular phenotypes: UBE3A (14), XRCC4 (26), TNIK (28), LRRIQ3 (38), MACROD2 (42), Cd36 (50), CHL1 (52), DOCK7/ANGPTL3 (64), PPAP2B (65), TRIB1 (77), MYO6 (79), TMEFF2 (85), GRIK1/CLDN17/CLDN8 (100), INSR (108), FLT1 (109), CNTNAP5 (115), FAM5c (119), FHIT (133), NRG3 (137), LZTS1/ATP6V1B2 (139), NEIL3 (141), RBPMS (143), ARHGEF7 (144), PHACTR1 (147), KCNN2 (149), POLR2M (154), DISC1 (159), ANKS1A (160), GRIK2 (163)

NAFLD and liver metabolism: RSPO3 (1), SLC2A2 (28), MACROD2 (42), TRIB1 (77), SLC46A3 (109), DDX60L (140), ATP8B1 (152)

Neurodegenerative and neurobehaviour

Alzheimer's disease: ZNF224 (10), CD33 (13), RRAS2 (20), STK24 (20), PPAPDC1A (21), UNC5C (36), rs7638995 (56), MAN2A1 (86), RP11-572M11.4 (104), RFC3 (107), DMXL1 (126), DISC1 (159)

Schizophrenia: TNIK (28), GRIK3 (66), FBXO11 (67), ITSN2 (68), STXBP6 (70), JRKL (78), CNTNAP5 (115), NRG3 (137), PALLD (140), TUSC3 (142)

Bipolar disorder: PRKAG2 (49), rs11123306 (117)

Autism: MACROD2 (42)

Attention deficit hyperactivity disorder: FRMD1 (4), FOXP1 (57), SLC6A1 (59), GRIK1 (100), PDX1/GSX1 (110), FHIT (133), ATP8B1 (152)

Major depressive disorder: EPN1 (109), FHIT (133), LZTS1/ATP6V1B2/SLC18A1 (139)

Autism, Attention deficit hyperactivity disorder, Bipolar disorder, Major depressive disorder and Schizophrenia combined: ELTD1 (37), GRIK1 (100)

Bipolar disorder and Schizophrenia combined: LRRIQ3 (38), ASTN2 (63), ERC2 (136), SPTLC1 (146)

Brain and central nervous system: RSPO3 (1), KIF25 (5), MACROD2 (42), RPN2 (45), SUMF1 (58), BICD1 (61), CRHR1 (94), KCNJ6 (102), ZNF326 (123), DISC1 (159)

Other neurological and neurobehavioural phenotypes: ARRDC4 (16), STK24 (20), FLG (32), LPHN2 (37), NXPH2 (39), SPOPL (39), MACROD2 (42), PLXNA4 (51), CHL1 (52), VGLL4 (59), DBC1 (63), LAMB4/NRCAM (70), NSF (94), FLT1 (109), USP12 (111), CNTNAP5 (115), DGKQ/GAK (122), LPHN3 (125), ARAP2 (127), KCNIP4 (128), COBL (130), FHIT (133), TUSC3 (142), GTF2E2 (143), PHACTR1 (147), FHOD3 (148), TOX3 (157), CNTNAP4 (158), DISC1 (159), GRIK2 (163), ASCC3 (163)

Autoimmunity inflammation and infectious diseases: FRMD1 (4), TTLL2 (4), RAB38 (19), RPS6KA4 (23), LPXN/CNTF (24), FLG (32), NEGR1 (38), MACROD2 (42), FRMD4B (56), LINGO2 (62), DBC1 (63), TRIB1 (77), MAML2/JRKL (78), PLCL2 (84), TMEM232 (86), RUNX1 (101), DYRK1A (102), USP12 (111), ANXA3 (124), COBL (130), UBAC2/GPR18/GPR183 (135), VEGFC (141), DAPK1 (145), NEDD9 (147), ATP8B1 (152), CYLD (157), CNTNAP4 (158), UHRF1BP1 (160)

Cancer: ECHD1 (1), "ADCY2 (2), PAPD7 (2), LPXN (24), CHL1 (52), ITPR1 (58), TEAD4 (60), BICD1 (61), MAML2 (78), STXBP4/COX11 (92), BACH1 (100), GRIK1 (100), RUNX1 (101), Zbtb20 (104), BRCA2 (106), SFPQ (114), TSN (116), LGR6 (118), UBAC2/GPR18/GPR183 (135), DAPK1 (145), TOX3 (157), DISC1 (159), ANKS1A (160)

Height: SHOX2 (30), PDIA4 (53), FBLN5 (71), SYN3/TIMP3 (75), MAML2 (78), SENP6 (79), FER (86), FBXW11 (88), SLIT3 (89), TMEM100/MMD (91), INSR (108), ZCCHC6 (145), ANKS1A (160)

Renal function: RSPO3 (1), SLC22A12 (23), CST9 (43), PRKAG2 (49), HLF (91), GRIK2 (163)

Hematology: NEGR1 (38), PLCB4 (41), SHH (47), PRKAG2 (49), Cd36 (50), STXBP6 (70), HSD17B6 (73), EPHB1/PPP2R3A (80), MYH15 (103), PCGF3 (122)

Bone: RSPO3 (1), CHL1 (52), SOST (93), CRHR1 (94), IDUA (122), ERC2 (136), PHACTR1 (147), CYLD (157)

Eye: POSTN (29), CTSS (33), SRC (45), SHH (47), SYN3/TIMP3 (75), FAM84B (77), MAML2 (78), INSR (108), FHIT (133), NRG3 (137)

Others: STK24 (20), MUC2 (22), RAP1GDS1 (36), ELTD1 (37), NXPH2 (39), ITPR1 (58), SLC6A1 (59), BICD1 (61), PPAP2B (65), PRIM1 (73), VAV1/EMR1 (81), ACE (95), C3Orf38 (99), RUNX1 (101), INSR (108), RNF212 (122), ANXA3 (124), LPHN3 (125), FHIT (133), SPRY2 (134), LZTS1 (139), TUSC3 (142), ARHGEF7 (144), GRIK2 (163)

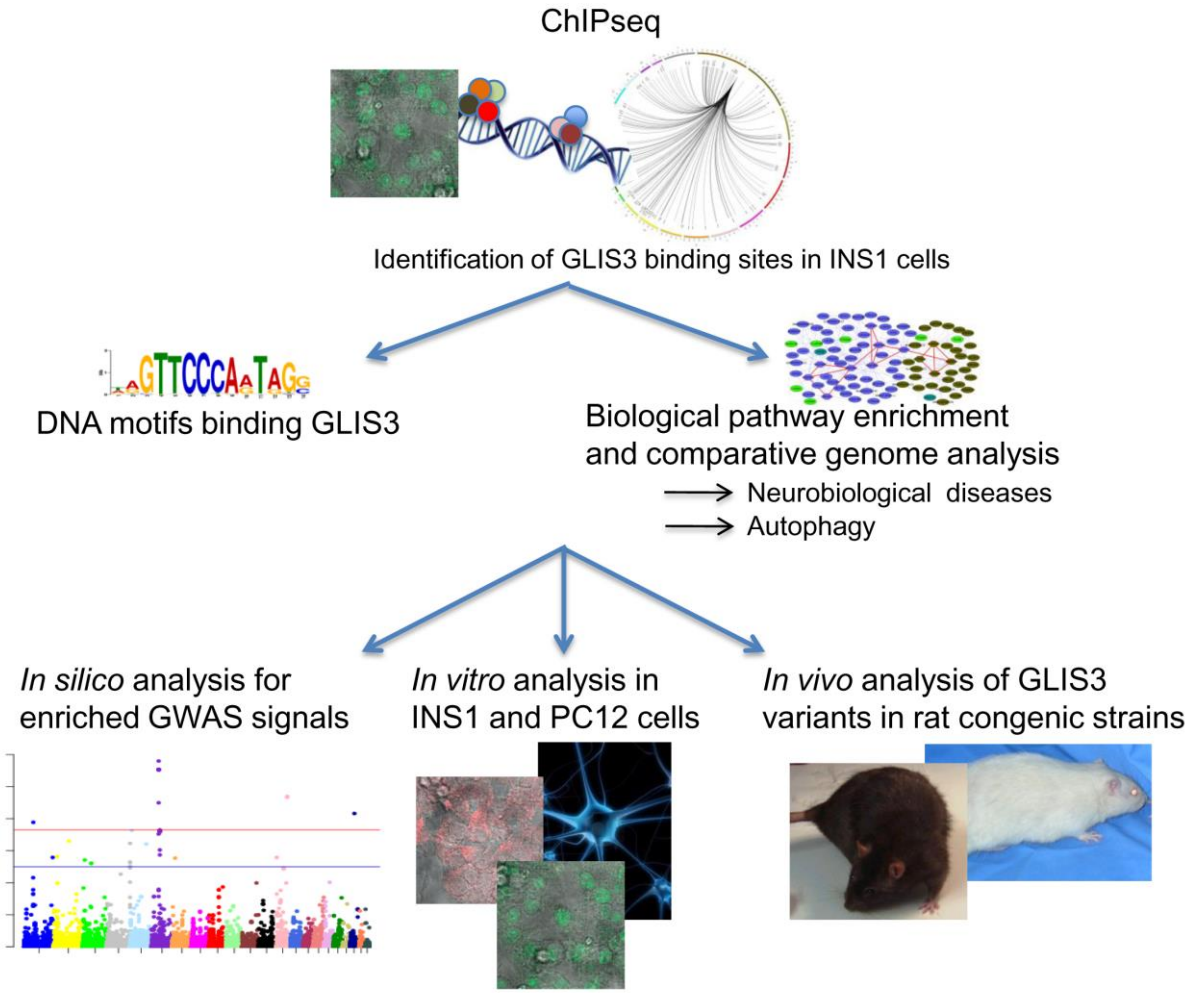

Fig. 1

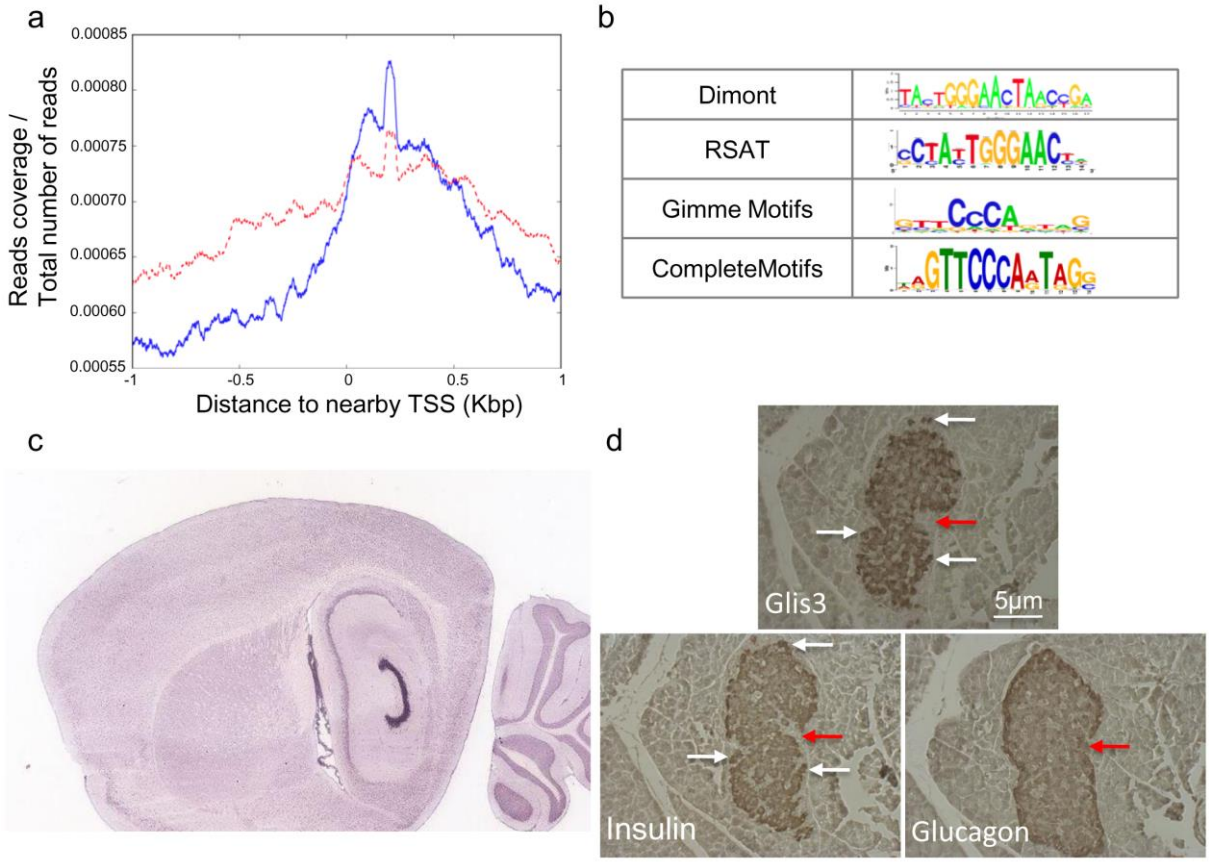

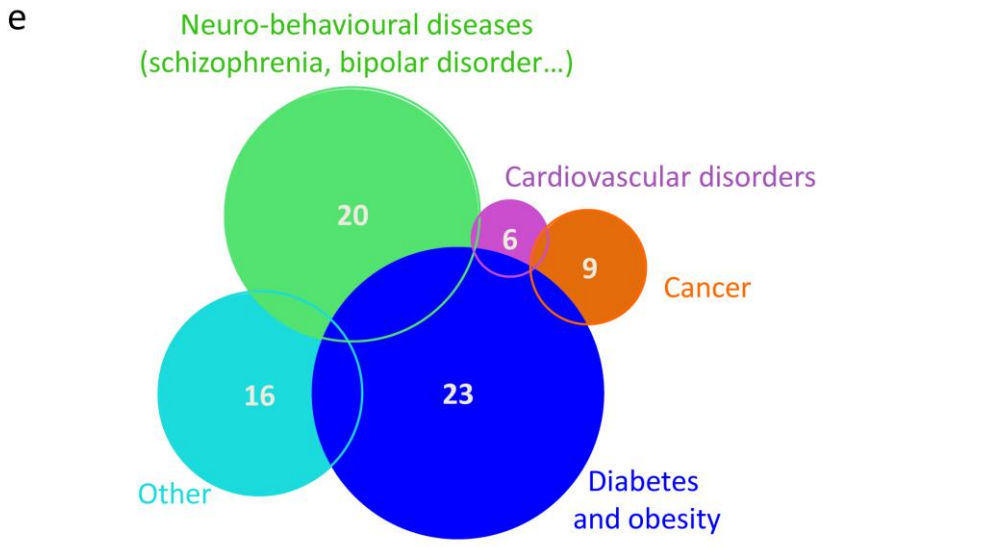

Fig. 2

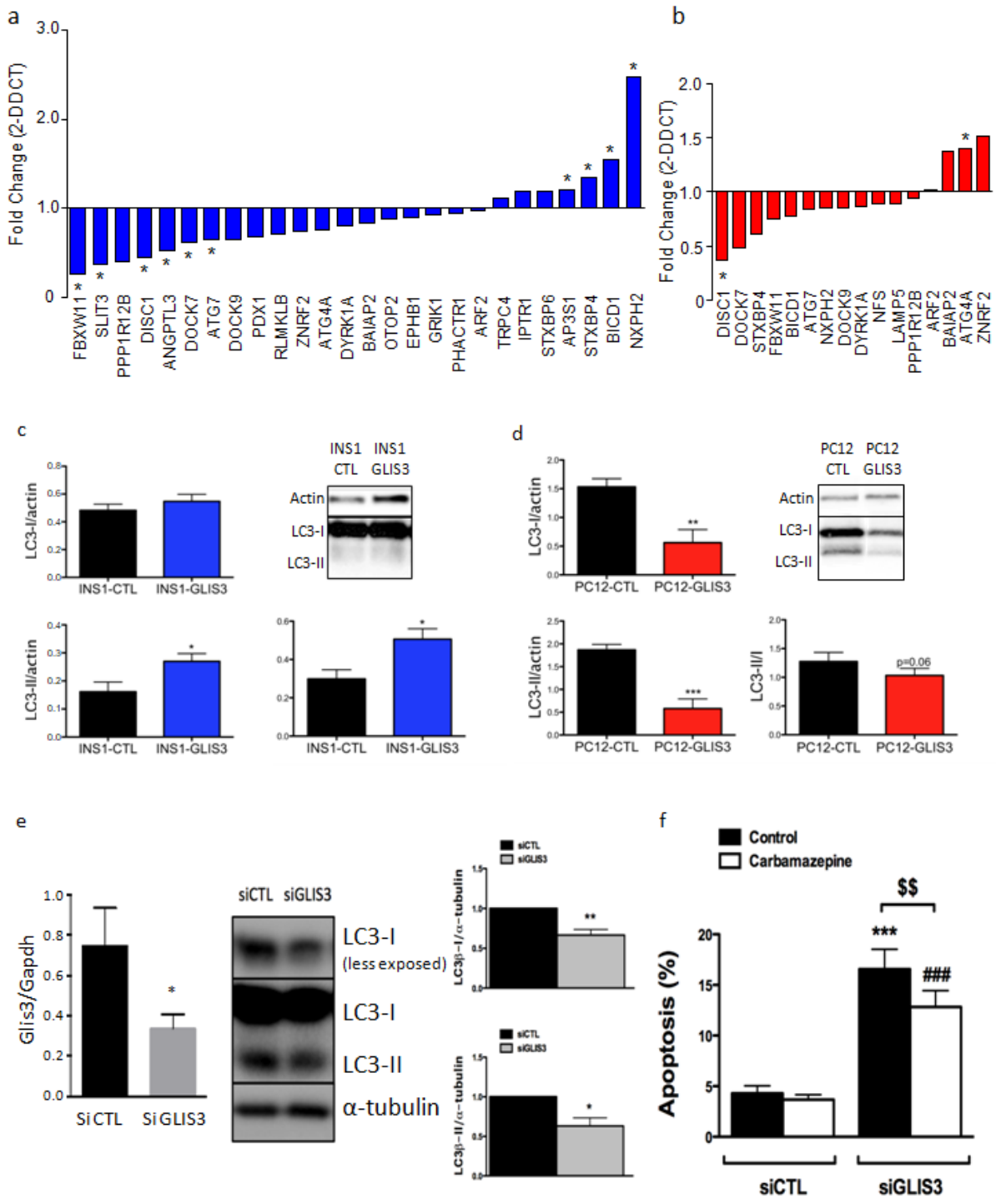

Fig. 3

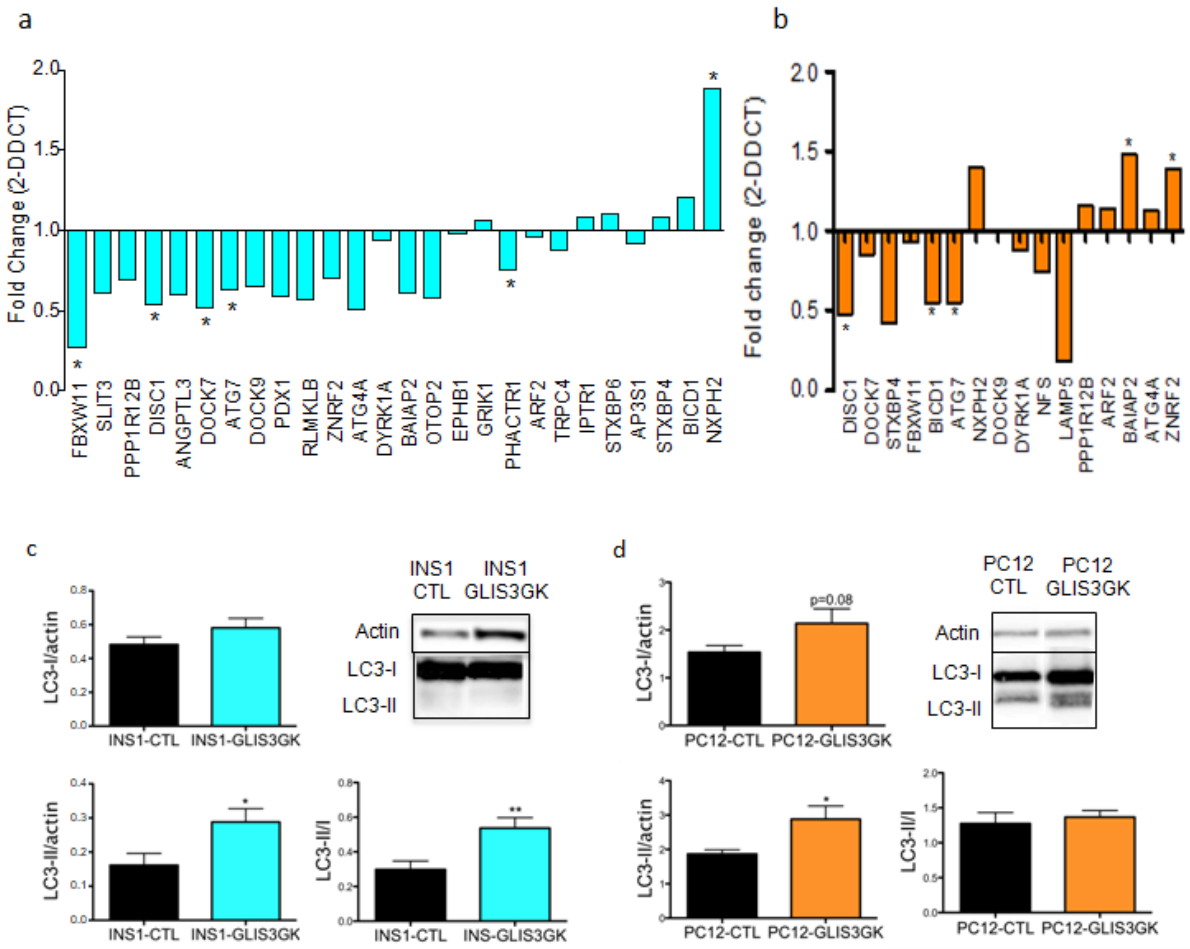

Fig. 4

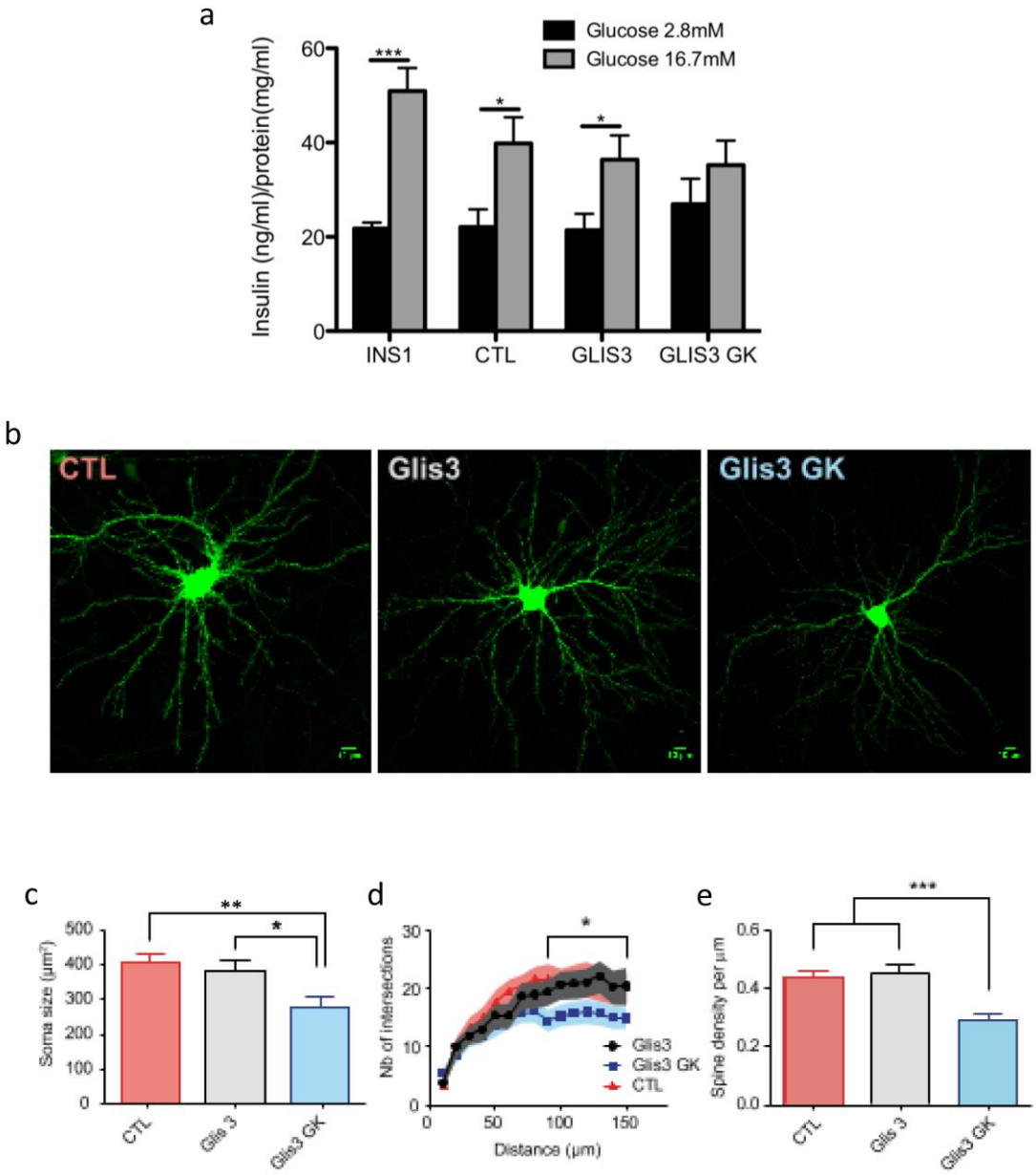

Fig. 5

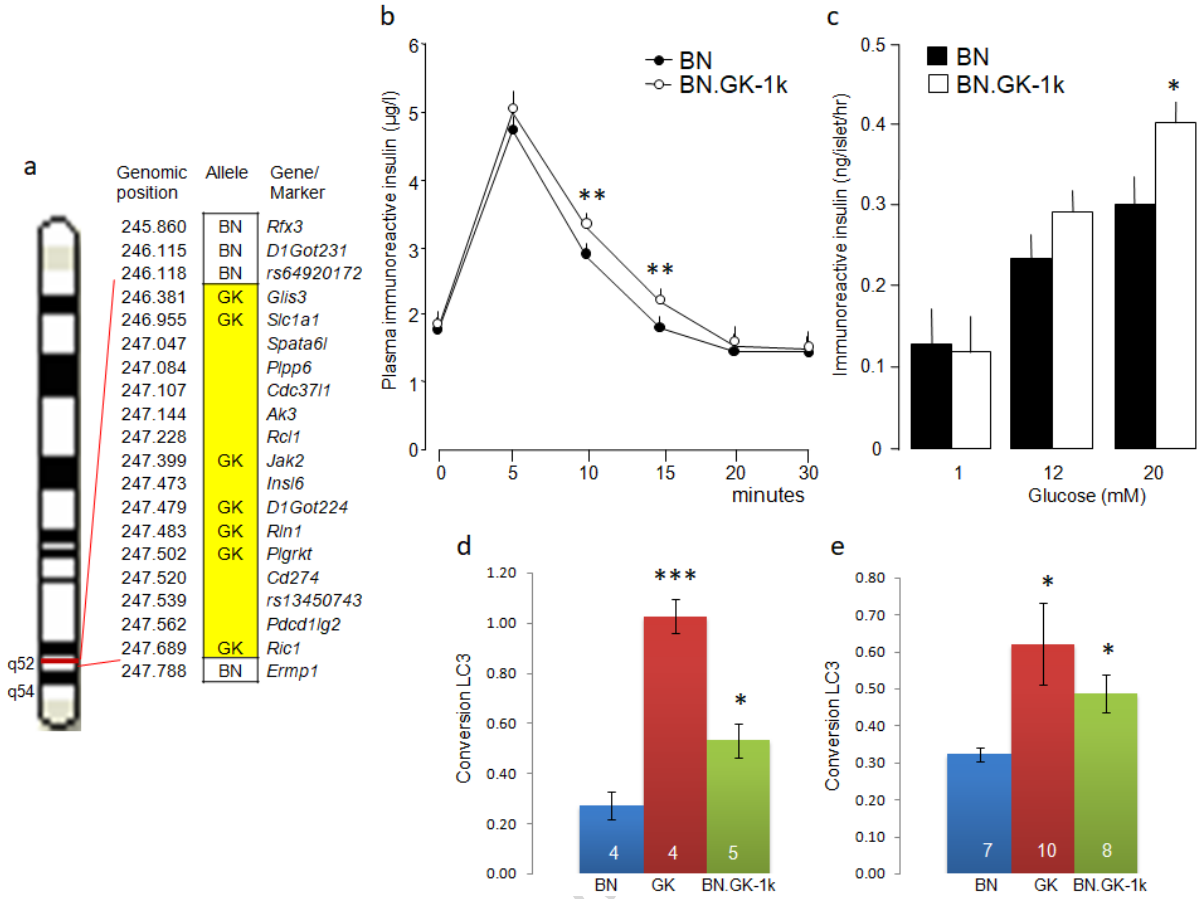

Fig. 6

Highlights

- GLIS3 binding sites in insulin secreting cells share the motif wrGTTCCCArTAGs
- GLIS3 controls the expression of genes involved in autophagy and neuron function
- *Glis3* sequence polymorphisms in the diabetic GK rat alter β-cell function
- *Glis3* variants in the GK rat modify neurogenesis in hippocampus neurons